**Naval Research Laboratory**

**Washington, DC 20375-5320**

NRL/MR/5341--95-7794

# Preliminary Study of Some Antenna Elements Which Have Potential Usefulness as Ultrawideband Radiators

S.N. SAMADDAR

*Radar Analysis Branch*
*Radar Division*



November 24, 1995

# REPORT DOCUMENTATION PAGE

*Form Approved*
*OMB No. 0704-0188*



| 1. AGENCY USE ONLY (*Leave Blank*) | 2. REPORT DATE | 3. REPORT TYPE AND DATES COVERED |
|---|---|---|
| | November 24, 1995 | Interim |

**4. TITLE AND SUBTITLE**

Preliminary Study of Some Antenna Elements Which Have Potential Usefulness as Ultrawideband Radiators

**5. FUNDING NUMBERS**

PE - 61153N
PR - LR021-05-RH

**6. AUTHOR(S)**

S.N. Samaddar

**7. PERFORMING ORGANIZATION NAME(S) AND ADDRESS(ES)**

Naval Research Laboratory
Washington, DC 20375-5320

**8. PERFORMING ORGANIZATION REPORT NUMBER**

NRL/MR/5341--95-7794

**9. SPONSORING/MONITORING AGENCY NAME(S) AND ADDRESS(ES)**

Office of Naval Research
800 North Quincy Street
Arlington, VA 22217-5660

**10. SPONSORING/MONITORING AGENCY REPORT NUMBER**

**11. SUPPLEMENTARY NOTES**

**12a. DISTRIBUTION/AVAILABILITY STATEMENT**

Approved for public release; distribution unlimited.

**12b. DISTRIBUTION CODE**

A

**13. ABSTRACT** (*Maximum 200 words*)

A preliminary investigation is conducted on the selection of antenna configurations which have potential to be ultrawideband (UWB). Each configuration is summarized. This includes discussions of new results that are byproducts of the study, conclusions that are drawn from the survey, and recommendations that are made which are predicated on the research. With regard to approaches for characterizing UWB antennas, two overriding conclusions emerged from this effort: (1) the philosophical maxim, "the proof of the UWB antenna is in its short-pulse behavior," should be implicit in any study, and (2) each campaign should be a synergistic merging of theoretical, numerical, and experimental methods. Based on the capability to enhance existing knowledge and understanding of the performance of UWB antennas, this study recommends the following topics be studied in greater detail: loaded dipoles, flared and notch antennas, helixes and spirals, fat antennas, arrays with mutual coupling, the possible reduction of phase variation in log-periodic antennas, wide-angle biconical antennas, and antennas that are suitable for impulse radiation.



**14. SUBJECT TERMS**

Ultrawideband
Transients
Short pulse
Radiation
Antenna

**15. NUMBER OF PAGES**

37

**16. PRICE CODE**

| 17. SECURITY CLASSIFICATION OF REPORT | 18. SECURITY CLASSIFICATION OF THIS PAGE | 19. SECURITY CLASSIFICATION OF ABSTRACT | 20. LIMITATION OF ABSTRACT |
|---|---|---|---|
| UNCLASSIFIED | UNCLASSIFIED | UNCLASSIFIED | UL |

NSN 7540-01-280-5500

Standard Form 298 (Rev. 2-89)
Prescribed by ANSI Std 239-18
298-102

## CONTENTS


1.0 INTRODUCTION . . . . . 1

2.0 DIPOLES . . . . . 2

3.0 LOADED DIPOLES . . . . . 3

4.0 FLARED AND TAPERED RADIATORS . . . . . 4

5.0 HELICAL AND SPIRAL ANTENNAS . . . . . 5

6.0 FAT ANTENNAS . . . . . 6

7.0 WIDE-ANGLE BICONICAL ANTENNAS . . . . . 7

8.0 ANTENNA ELEMENTS FOR IMPULSE RADIATION . . . . . 7

9.0 HARMUTH'S LARGE CURRENT RADIATOR . . . . . 8

10.0 POSSIBLE REDUCTION OF PHASE VARIATION OF LOG-PERIODIC ANTENNAS . . . . . 9

11.0 ARRAYS AND MUTUAL COUPLING . . . . . 9

12.0 NUMERICAL APPROACH TO SOLVING ANTENNA PROBLEMS . . . . 9

13.0 CONCLUSIONS AND RECOMMENDATIONS . . . . . 10

13.0 ACKNOWLEDGEMENT . . . . . 12

14.0 REFERENCES . . . . . 12

APPENDIX A—Biconical Antennas with Unequal Cone Angles . . . . . 17

APPENDIX B—Radiation Field of Helical Antennas with Sinusoidal Current . . . . . 33

# PRELIMINARY STUDY OF SOME ANTENNA ELEMENTS WHICH HAVE POTENTIAL USEFULNESS AS ULTRAWIDEBAND RADIATORS

## 1.0 INTRODUCTION

The purpose of this preliminary study is to obtain information about the various characteristics of different antenna elements that are considered very wideband or ultrawideband (UWB) and to understand and explain to some extent the how and the why of broadbandedness. The UWB behavior of a radiator is well defined by its short-pulse response. In an ideal situation, when excited by a short-pulse, an UWB antenna should be capable of radiating a distortionless replica of that pulse. Since most antenna analyses in the literature are in the frequency domain and apply narrowband concepts and measures, one shall have to determine how much of this is appropriate or can be extended to understanding what makes a radiator ultrawideband. The word "short-pulse" used here is a relative term. As discussed below, the term UWB also does not have a fixed range. However, for a given UWB system it is desirable to have at least one associated "short-pulse," which can pass through (or interact with) the UWB system with minimum distortion. It is in this sense the word "short-pulse" will be used in this report.

Before proceeding further, we digress momentarily to say a few words about terminology like wideband, ultrawideband, bandwidth, etc. First define the fractional bandwidth $B_F$ of a system or device. If a system operates well for a range of frequencies, having $f_u$ and $f_l$ as the upper and lower values, respectively, then $B_F$ is defined by $B_F = (f_u - f_l)/f_c$, where the center frequency $f_c$ is the mean value of $f_u$ and $f_l$ (that is, $f_c = (f_u + f_l)/2$). How $f_u$ and $f_l$ are chosen is quite arbitrary and generally depends on the desired performance of the system under consideration. A multiplication of $B_F$ by 100 gives the percentage bandwidth. By defining the frequency ratio $f_u/f_l$ as $N$, one finds that $B_F = 2(N - 1)/(N + 1)$ or $N = (2 + B_F)/(2 - B_F)$. After searching the literature ([1]-[5]), it is clear that no commonly or widely accepted definitions of wideband and ultrawideband exist. However, we suggest that any definitions one wishes to make should, perhaps, have been taken after the completion of analytical and experimental studies of antennas which have potential of becoming UWB, remembering that "the proof of an UWB antenna is in its short-pulse behavior." In other words, the practical limitations on the UWB performance of an antenna should also play a role in the adoption of any definition.

To achieve the above mentioned goals, we reviewed the existing literature on wideband antennas and related subjects. The intent of the review was to develop the analytical background necessary for drawing enlightened opinions and accurate technical judgements on UWB antennas, rather than merely undertaking a cursory survey of the introductions and conclusions of various research papers. Consequently, this report is an "analytical" review. Although complete solutions of new problems

Manuscript approved October 12, 1995.

from beginning to end were not objectives of the review, in some cases new results were generated during this preliminary investigatory process. These results are summarized in subsequent sections.

Specifically, this report discusses the following topics: dipoles, loaded dipoles, flared and tapered radiators, helical and spiral antennas, fat antennas including wide-angle cones, antennas for impulse radiation (IRA), Harmuth's large-current radiator, UWB version of log-periodic antennas, arrays and mutual couplings and numerical approach to solving antenna problems. The last section draws conclusions from existing research of wideband and UWB antennas and makes recommendations on how these antennas should be investigated analytically, numerically, and experimentally. Finally in the appendices, we present briefly some analytical results, that are by products of this study.

## 2.0 DIPOLES

Although a thin dipole, a low gain radiating element, usually is not considered to be a broadband (or wideband) antenna, a familiarity with its radiation mechanism and characteristics might lead one to better understand how a wideband or even an ultrawideband (UWB) radiator should perform.

In previous studies [6,7] using a simplified model of a thin dipole, we learned the mechanism of radiation when the dipole is energized by a short pulse. For a single-cycle pulse, we found that the pulse was distorted and stretched in time due to radiation from the end points (in addition to the feed point) of the dipole. In addition, the reflections of current from the end points are followed by radiation from the feed at separate intervals of time. Such behavior can be explained more clearly with reference to Fig. 1, showing a vertical dipole excited by a single-cycle sinusoidal voltage pulse $\sin \omega_0 t$ of duration $T(=\omega_0/2\pi)$ at the feed point $O$. The observation point $P$ is at a far distance from the antenna and therefore the lines $AP$, $OP$ and $BP$ are parallel for all practical purposes. The first pulse arriving at $P$ originates from $O$ and travels along $OP$. This pulse of duration $T$ is the retarded replica of the exciting input voltage, i.e. $\sin \omega_0 t^*$, where $t^* = t - r/c$, $t$ being the instantaneous observation time. The second pulse reaches $P$ after a time delay $h(1 - \cos \theta)/c$ after the arrival of the first pulse. This second pulse travels the path $OAP$. The third pulse arrives at $P$ delayed by $h(1 + \cos \theta)/c$ from the first one. This third pulse traverses the path $OBP$. Both the second and the third pulses are 180° out-of-pulse with respect to the first pulse. As soon as the radiations take place from the end points $A$ and $B$ (corresponding to the second and third pulses, respectively), the currents are reflected back to the feed point $O$ from both $A$ and $B$. Since the distances $OA$ and $OB$ are the same in this example, these two reflected currents (or voltages) are in phase and radiate simultaneously from $O$ along the ray $OP$ reaching the observer at a time $2h/c$ delayed from the first one. Note that each of these pulses has a time duration $T$. It should also be pointed out that in an actual situation a transmitting dipole will radiate many signals (although with diminished amplitudes), instead of four distinct signals. The reason for this is that the zero-order approximation allows the transmitter current to be reflected back to the feed point only once from each end point.

When a similar dipole is used as a receiving antenna, each of the above mentioned distinct incoming pulses will induce voltages in four different ways at the input of the matched receiving dipole. This study of a simple radiating structure (that is, a thin dipole) teaches us the following:

i. An infinitely long dipole can radiate the exciting input pulse without any distortion, since the distortion is caused by the radiations from the discontinuities (here, the end points). Therefore, if by some artifice, the reflections and radiations from the end points of a finite antenna could have been prevented, the exciting input pulse would have radiated without any distortion. In other words, a relatively narrowband dipole would have performed as an UWB radiator.

ii. As we know from our familiarity with the frequency-domain analysis of a given narrowband antenna, the primary reason for its narrowband behavior is the rapid variation of its input impedance with frequency. We, therefore, infer that the cause of such variations is mainly due to the reflection of the exciting signal from the discontinuities of the radiator.

The above observations then suggest that if either by some artificial means or by suitable shaping of an antenna the reflection from its discontinuities can be totally eliminated or at least minimized, the antenna becomes UWB. Since radiation (as well as reflection) takes place from the discontinuities of a radiator, one can then infer that if both current and voltage along a given antenna can be represented by continuous functions within an "open interval" on the antenna surface, neither radiation nor reflection will occur from such an interval. This does not, however, mean that this continuous open interval from the antenna surface can be removed without affecting the performance of the antenna. In other words, since all antennas are finite and have discontinuities, the exciting pulse cannot be radiated without any distortion.

## 3.0 LOADED DIPOLES

The use of loaded dipoles for the prevention of reflections is not a new idea. It appears that it was first suggested and tested by Hallén [8], which might have prompted Wu and King [9] to provide the appropriate theory. As noted below, the reflectionless behavior of the antenna makes it a traveling-wave type radiator, which is in general broadband [10]. The introduction of lossy materials inevitably lowers the efficiency, however the overall efficiency in a transmitting system is often sacrificed for improvements in its broadband and directional properties. It is also recognized that efficiency may not be the most important factor in a receiving antenna for which broadbandedness, directivity, and the simplicity of the system are the most desirable features.

It may be noted that most of work on the loaded antenna is confined to resistive loading, which reduces efficiency. The possibility of reactive loading (in particular, capacitive loading), although mentioned by Hallén [8], lacks appropriate attention except the work reported in [11]. This aspect of antenna loading should be explored, since apparently there is no loss of energy incurred. Consequently, the efficiency of a reactively loaded antenna is expected to increase when compared to a resistively loaded one.

Some recent works [12] show both experimentally and theoretically that a resistively loaded antenna, excited by a short pulse, is capable of radiating the same pulse without any appreciable distortion. For a resistively loaded dipole, the theory [9,12] assumes that the antenna is made of resistive material so that its internal impedance per unit length $Z_i$ is proportional to the inverse of $(h-|z|)$, where $z$ is the distance measured along an antenna having a total length $2h$. They then showed that the current distribution on such a loaded dipole behaves like a traveling wave of the form $(h-|z|)e^{ik|z|}$, where $k = \omega/c = 2\pi/\lambda$. By using this current, they computed approximately the radiated field as well as the power. This distribution of current makes it vanish at the end points, but the voltage, although small, does not vanish. However, Hallén [8] claimed that his experimental results for a capacitively loaded dipole showed that both current and voltage vanish near the end of the dipole. This prompted us to assume a different form of internal impedance which goes to infinity strongly as the end of the dipole is approached. When we used this form of the internal impedance distribution, we were able to obtain an analytical expression of the current distribution in terms of a confluent hypergometric function. Our preliminary analyses showed that in this situation both the current and voltage near the end of the antenna go to zero faster than the example considered in [9]. This model then is a good candidate for a future detailed study.

Finally, we would also like to mention our "in-house work" which indicates that the loss in efficiency of some resistive loading may be reduced. For example, experiments show [14] that the radiation pattern of a horn antenna consists of a forward lobe, which may be called the desirable lobe or gain-lobe, and some undesirable backward lobes. The latter might be generated by the horn's discontinuous edge. However, when the end surface of the horn was "extended by lossy tapered metalized mylar strips," the back-lobes disappeared without distorting the size and shape of the forward lobe. This shows that the antenna-gain was not reduced visibly. Thus it may be inferred that the antenna was matched to free space by the process just described. This method should also be tried with other antennas excited by short-pulse inputs, and the associated experiments should determine gain, beamwidth, efficiency, etc.

## 4.0 FLARED AND TAPERED RADIATORS

It has been analytically argued for the thin dipole that radiation emanates from the end points, from geometric discontinuities including the feed point, and from reflections back to the feed point from these discontinuities [6]. As a general rule, it seems evident that the less sharp an antenna's surface the smaller the reflections and the broader its bandwidth. Therefore, as noted earlier, increased bandwidth can be achieved by shaping the antenna to a smoother surface, thereby reducing reflections to a large extent. Any antenna that reduces reflections from its geometric discontinuities is a candidate for a "good" UWB antenna (such as TEM horns). Examples of shaping are antennas that widen (flare) or narrow (taper) from the feed, of which the flared notch is a special case. A *V*-antenna is the simplest example of a flared radiator. Such shaped antennas are made from waveguides, wires, tapered slots, etc. For the flared notch, the feed point has the narrowest gap and supports radiation at the highest frequency; whereas the open end has the largest separation and radiates the lowest frequency. Discussions of other radiators of this category are found in [15]. Reference [16] shows the performance of such an antenna under the name, "Rudimentary Horn," which previously was investigated both theoretically and experimentally. The theory in [16] was developed for the radiation field produced by a symmetrical rudimentary horn having exponentially curved radiating elements. Although their experimental work is satisfactory, according to the authors the theory is inadequate.

Generally, the geometrical shape of these radiators makes mathematical analysis difficult. Consequently, the literature avoids analytical treatments of these antennas in favor of experimental and numerical methods, which unfortunately provide little understanding of the underlying mechanisms of radiation from such structures. Therefore, it is inadvisable to analyze flaring via a strictly numerical-experimental approach without the accompanying fundamental analytical studies. Although analytical approaches are admittedly more difficult and typically do not produce immediate results, they are far from impossible and should be an integral part of any solution. In this vein, one should investigate simpler antennas like wires and horns with various types of flaring (polynomial, exponential, V which has linear flaring, etc.).

With regard to theoretical analysis, we made an attempt to analyze radiation from the flared antenna by assuming a suitable traveling-wave current distribution along the antenna surface and formally obtained an expression which is related to the far field of the vector potential. This analytical expression consists of a complicated integral which cannot be evaluated in closed form. We left the problem at that point as a topic for future study when some reasonable approximations to the integral, as well as evaluation by computer, may be made. In addition, an alternative method of approach for solving such problems using Schelkunoff's local eigenmode expansion method [17], subject to some appropriate approximation, is worthy of consideration. This method is expected to provide a better analytical expression for the current distribution along the curved surface.

From the existing literature [15], it appears that since different frequencies radiate from different parts of flared radiators or tapered-slot antennas, the phase center of such radiating elements will change with frequency, thereby making them dispersive. Flared or tapered antennas are judged wideband based on their performance characteristics in the frequency domain; however, a true picture of their wideband character can be revealed by studying their short-pulse responses both analytically and experimentally.

## 5.0 HELICAL AND SPIRAL ANTENNAS

The two types of helical antennas are designated "normal mode" and "axial mode" [15,18]. For a normal-mode antenna, the circumferential length of one turn multiplied by the number of turns is much shorter than a wavelength, and the maximum radiation takes place in the direction perpendicular to the axis of the helix (also known as "side-fire" or "broadside"). On the other hand, if the circumference of the helix is approximately one wavelength and if it has several turns per wavelength, the dominant component of the current on the helix behaves like a traveling wave along the helical wire and travels with a speed approximately equal to that of light. The energy flows along the surface that bounds the helix in the direction of the helical axis and is radiated from the discontinuity at the end. This type, known as the axial-mode helix, has a beamlike radiation pattern off the end of the helix. This pattern is essentially circularly polarized in the neighborhood of the axial direction. The radiation from an axial-mode helix is called either end-fire or back-fire. It has been found experimentally that if the diameter of the helix remains constant, the bandwidth of an axial-mode helix may be 40% to 50%. On the other hand, if the helix is tapered, its bandwidth may be 133% [15,19,20].

An exact theory of a finite helical antenna is very difficult to handle as a boundary value problem, and therefore the actual current distribution along the wire is unavailable. Consequently, various authors [15,18,21] have assumed some approximate current distribution, generally a traveling-wave type, and have calculated the radiation pattern analytically. Of these authors, many citations of Kornhauser [21] appear in the literature. Unfortunately, his paper has some errors, and consequently his results are not valid for all directions. Since we are not aware of anybody who might have corrected them, we made an effort to repeat his analysis correctly in the frequency domain. Our derived model can be used to investigate the short-pulse response of this helical antenna.

With regard to spiral antennas, it was found [22-24] that if the shape of the antenna could be completely described by angles, its performance would have to be independent of frequency. The theory for such antennas assumes infinite structures. An equiangular spiral on a plane belongs to this category. To make infinite structures more practical, the designs are made so that the current on the structure decreases with increasing distance from the feed terminals and so that the reflections are minimized. If after a certain point the current along the structure is negligible, then the structure beyond that point to infinity can be removed with a negligible effect on the performance of the antenna. The lowest frequency that the spiral can transmit is that for which the current at the truncated point becomes negligible. On the other hand, the largest transmission frequency depends on the cross-sectional dimension of the feed transmission line where the line ceases to appear as a "point" (usually $\lambda_{min}/8$, where $\lambda_{min}$ is the wavelength of the highest frequency). In this way, a very large bandwidth having frequency ratio on the order of 100:1 (or more) is achievable.

Unfortunately however, such frequency-independent antennas have phase centers that depend on frequency, and therefore their responses to a short pulse are highly dispersive. One then may inquire, "Are there ways to modify such structures so that their short-pulse characteristics becomes less dispersive?" We shall address this point briefly in a later section.

In summary, we were motivated to pursue this type of antenna because its radiation is very directed and the small reflections from the discontinuity at the end make it UWB. Moreover, existing theory inadequately treats the feed system, and a reasonable analytical characterization of the frequency-dependent, traveling-wave propagation constant $ß(\omega)$ in the current $I(s, \omega)$, where $I(s, \omega) = I_o(\omega)\exp(-iß(\omega)s)$, along the helix apparently does not exist. Typically, only experimental values of ß are available at discrete $\omega$. Clearly, an analytical expression of ß is needed for analysis of UWB signals. Unresolved issues on the helix that might be answered include (1) its short-pulse behavior for the assumed model of $ß(\omega)$ given in [15], (2) a reasonable analytical model of $ß(\omega)$, (3) approximate analytical solutions for $I(s, \omega)$, (4) good matching between an idealized feed network and a helix, (5) the effect of a helix on short-pulse inputs, and (6) the definition and purity of circular polarization. Since each issue is difficult, to undertake all of them would be overly ambitious. In fact, we believe that items (2) through (6) are not priorities but that item (1) is worth pursuing.

## 6.0 FAT ANTENNAS

Although a thin wire (thin cylindrical conductor) is a narrowband antenna, a fat cylindrical dipole behaves like a wideband radiator. In general, fat antennas are broadband. In addition to the fat cylindrical dipole, members of the fat-dipole family include wide-angle conical (or biconical), spherical, and spheroidal antennas. Theoretical analyses of a finite, fat cylindrical dipole and a wide-angle cone are very difficult; whereas exact analytical field expansions for spherical and spheroidal antennas can be obtained with less effort [25,26]. Unfortunately, even these exact solutions do not necessarily provide the underlying physical understanding of the antenna's characteristics for the UWB range of frequencies.

Those who are familiar with the problem of scattering from spheres and spheroids know that the representation of the scattered field converges very slowly as the frequency increases. Analogous mathematical difficulties are encountered with spherical and spheroidal antennas. In scattering problems, resonance scattering may help in identifying whether the scattering object resembles a sphere or spheroid. Similarly, a radiator may be identified from its resonance radiations. Thus resonance radiations are important phenomena for investigation. Most scattering problems are worked out in the frequency domain, because transient scattering and radiation problems, which require inverse Fourier transforms, are more difficult to handle. However, some attempts [27,28] have been made for some limiting cases, such as for very low and high frequencies.

One may suggest, "Why not use a powerful computer to calculate numerically the above-mentioned slowly convergent series associated with radiations from spherical and spheroidal antennas?" Although this is certainly a good notion, one should not use numerical methods blindly without testing them against analytical or experimental results for some known cases. Consequently, numerical analysis is a worthwhile task only after some insight is gained through analytical means for some limiting cases. Such analytical means may consist of exploring the approach by the Russian Physicist Fok [29], who transformed the Helmholtz wave equation to a parabolic one by some suitable approximation, which had been used to study radio wave propagation over the spherical earth. Further investigations are, therefore needed for better understanding the short-pulse responses from spheroidal antennas. Because of their smooth shapes, spheroidal antennas are expected to have better broadband characteristics than a fat cylindrical dipole. So far, we have reviewed the works cited in [25,26,27].

Since there are large number of resonance radiations associated with fat antennas than their thin counterparts, one may infer that these large number of resonances are responsible for making a fat antenna broadband.

Finally, wide-angle conical antennas are discussed in the following section, since we have studied them in more detail.

## 7.0 WIDE-ANGLE BICONICAL ANTENNAS

When one searches the recent literature (books, conference proceedings, etc.) for the names of very-wideband or ultrawideband (UWB) antenna elements that are nondispersive, biconical antennas are most frequently cited. Axially symmetric bicones, excited by a symmetrically fed source at the apex, radiate axially symmetric electromagnetic fields. This property of a bicone may not make it a good candidate for radar applications. However, analyses of TEM horns, V-conical antennas, triangular plates or bow-tie antennas, etc, which are often used for launching impulse radiations, require some knowledge of a biconical antenna's characteristics. Furthermore, some conical radiators, which are made geometrically asymmetrical (such as when the axes of two cones are inclined to each other), radiate axially non-uniform electromagnetic waves. These unsymmetrically radiating cones may find their applications in a modern UWB radar antenna system. However, analyses of such asymmetrical conical antennas will not be easy to treat.

With the preceding thoughts as motivation, we studied the theory of biconical antennas in somewhat greater detail than the radiators discussed thus far. Initially, the works described in [30-38] were reviewed. During this process, we extended some of their analyses and obtained some new results. Some of these results are now briefly discussed to show the nature of our contributions.

Some recent papers discussing radiation from finite biconical antennas or finite TEM horns assume the existence of only TEM waves in the antenna region. They can in general also support TM waves, which become negligible, however, when the cone angles are wide. This point is clear only upon a careful reading of the papers by Smith [31] and Tai [32-34], justifying the study of these references. Both Smith and Tai obtained analytical expressions of the bicone's input impedance and showed it also depends on TM modes. Tai [34] was also able to cast the expression for the input impedance in a variational form. This variational form indicates that the influence of TM waves becomes negligible for the wider cone angles together with increasing frequencies. This result then suggests that finite wide-angle bicones behave like infinite cones for high frequencies. In other words, in the high-frequency limit, the input impedance of a finite cone approaches the characteristic impedance of the biconical antenna. Both Smith [31] and Tai [34] investigated the characteristics of biconical antennas with equal cone angles. We extended their work to include bicones having unequal cone angles. For bicones with unequal angles, we obtained expressions for the input impedance, its variational form, the far-field, and their high-frequency behaviors in the frequency domain.

We found that for a wide-angle electrically long bicone (i.e. in the high frequency region) the maximum radiation moves towards the surface of the cone instead of the broadside of the cone. The analyses of the biconical antenna with unequal cone angles are presented in Appendix A.

## 8.0 ANTENNA ELEMENTS FOR IMPULSE RADIATION

TEM-fed antennas play a dominant role in most of the UWB systems that have been studied and built. The system roughly consists of a source, a parabolic reflector, and feeds that connect the source and reflector. In particular, Baum and his associates [39] have developed and analyzed impulse radiating antennas (IRAs), where the source-fed elements may be TEM horns of different shapes, circular cones, etc. They have a newly designed system, located at Phillips Laboratory's High Energy Research Technology Facility (HERTF), which consists of four feeds (two pairs) that connect a source-fed lens and a parabolic reflector. To guarantee that the system operates in horizontal and vertical polarizations, the feeds for each pair are arranged so that the planes corresponding to each pair are perpendicular. The system's frequency band covers 50 MHz through

2 GHz, hence the fractional bandwidth is 190%. The high-frequency cutoff is limited by the 200-ps risetime of their 10-kV Bournlea pulser, and the low-frequency cutoff is determined by the size of the reflector (12-foot diameter). The source lens ensures that the TEM field at the reflector is a spherical wave.

Since an IRA is capable of launching UWB signals effectively, an understanding of IRA systems is essential. Before one can accomplish this goal, it is necessary to develop familiarity with the performance of an IRA's feed elements. With this in mind, we looked very briefly into the literature on these feed elements. Ideally, an appropriate feed element apparently is meant to launch a pure spherical TEM wave, so that the feed structure maintains a very broadband character. Although any antenna having finite size cannot support pure TEM modes, the influence of excited higher-order TM waves is significantly reduced by an appropriate choice of antenna dimension together with impedance matching. Therefore, most feed elements in the analyses of Baum and his associates are assumed to have infinite length, because they feel that such elements provide accurate characterizations of the electromagnetic behavior of their finite counterparts. This is the philosophical approach inherent in Baums conceptualization of IRAs.

After careful scrutiny, one can observe that the geometrical shapes of Baum's elements are special cases of cones or bicones, which were discussed in the preceding section. In Baum's analyses, as well as the analyses of other [40,41], of these infinitely long elements, the characteristic impedances and transverse fields that they support are calculated by repeated applications of conformal transformations, a specialized subject in complex variables. In addition, conformal transformations have been used in other radiation work to determine analytically the transverse electromagnetic modes in linearly tapered slot antennas [42], which apparently belongs to the family of notch antennas.

To date, we have spent little time on a detailed study of IRAs. Since these structures can be used in UWB antennas other than those mentioned above, it might be worthwhile devoting some time to understanding their performances and analytical behaviors.

## 9.0 HARMUTH'S LARGE CURRENT RADIATOR

This antenna [43,44] is made of a rectangular metal sheet which is connected via triangular section of metal sheet to a wire through which source voltage is applied. Absorbing material is also placed in an appropriate manner so that the radiation from this wire does not interfere with that from the rectangular plate. The principle of operation, according to Harmuth, depends on the absence of electric charges which give rise to the scalar potential $\Phi$. In other words, there is no capacitor formed by the antenna; thereby $\Phi = 0$. The scalar potential produces non-vanishing components of the electric field E in the near-zone. Harmuth finds this advantageous since the absence of these near-zone field components (since $\Phi = 0$) does not call for a high driving voltage of the power source. Harmuth finds also a second advantage of the large-current radiator, for which the assumption of the same current anywhere along the antenna is satisfied. However, for a conventional dipole antenna this assumption is not true. These are the basic principles upon which a large-current antenna operates and is designed.

We did not have time to study thoroughly these principles and theory of operation of this antenna. However, an apparent question surfacing our mind is not clearly explained. The spatially constant current along the antenna implies that the antenna is excited by a pulse consisting only of low frequency spectra. Whether the exciting pulse is a nonsinusoidal one, it can always be decomposed into Fourier spectral components. It, therefore, appears to us that these large-current antennas are limited to low frequencies and to low bandwidth.

In spite of the question raised above this large current radiator deserves more attention theoretically as well as experimentally.

## 10.0 POSSIBLE REDUCTION OF PHASE VARIATION OF LOG-PERIODIC ANTENNAS

As noted earlier, variable phase-frequency characteristics of frequency-independent antennas make them unsuitable for radiating short pulses, since the shape of the radiated signals are distorted severely. In this respect, if one could devise an arrangement which makes the phase-frequency relationship nearly linear and the gain factor of the antennas roughly constant, the distortion of the radiated short pulse would be reduced to an extent. Some investigations along this direction have been reported by Russian researchers [45]. In [45], they considered log-periodic antennas which consisted of a number of parallel linear dipoles placed in a certain fashion. It is not clear, however, whether their theory and technique are applicable to an antenna with a continuous surface, such as spirals. Nevertheless, it would be worthwhile effort to study the theory described in [45], so that the technique can be extended to other types of dispersive radiators. Unfortunately, at least three practical difficulties arise when dealing with the Russian literature: (1) gaining access to the reference, (2) translating it into English, and (3) the paucity of details in the exposition.

## 11.0 ARRAYS AND MUTUAL COUPLING

Many single-element radiators are low gain and lack the desired directive radiation. However, a convenient method of placing more radiation in a specified direction consists of arranging low-gain radiators in arrays so that the array's dimensions extend over many wavelengths relative to the center frequency of the transmitted signal's spectrum. The direction of maximum radiation is controlled by introducing appropriate phase shifts at the radiating elements. Through this procedure, called electronic scanning, the direction of maximum radiation is varied at will by changing electronically the relative phase-shift with frequency. Most array analyses are performed in the frequency domain for narrrowband signals, where an array can be designed to provide directive radiation with a narrow beam. Since both directivity and beamwidth depend on frequency, little is known about the performance of an array when subjected to a short-pulse signal. Clearly, many questions need to be answered for UWB signals. For example, "How should one define the beamwidth of the radiated field?" Should the time delay between adjacent elements be dependent on the carrier frequency, if any, of the short pulse? If not, then how would one select a time delay? In order to answer these questions, it is necessary to investigate the characteristic behaviors of a given array when it radiates or receives a short pulse.

Furthermore, when antenna elements are placed in close proximity, as in an array, interactions between them affect the impedances "seen" by the feed system at the driving points. The terminal impedance (or input impedance) of a dipole with a reflector, a situation equivalent to a pair of dipoles, is also affected in a similar manner. Such behavior, due to mutual coupling between the radiators, will definitely influence the bandwidth of the system. In order to have better insight, one should first investigate the characteristics of two parallel dipoles which are excited by a short pulse. This study should show how the radiated field behaves, how much it is distorted, etc. Finally, the study may be extended to an array of dipoles.

## 12.0 NUMERICAL APPROACH TO SOLVING ANTENNA PROBLEMS

Only a handful of antenna elements exist which can be subjected to complete analytical investigation. Even for some apparently simple antenna configurations, suitable approximations are necessary for obtaining insight into certain salient characteristics of the antenna under consideration. However, not all useful antenna configurations are simple, and it is also necessary to know the antenna behavior for which the above-mentioned approximations are not permissible. In these

situations, it is appropriate and advantageous to use numerical methods and computers. But like any approach, numerical analysis has its disadvantages, and they are:

i. If there are errors in numerical computations (which may be due to programming, roundoff, etc.), one may not be aware of them, and it may be a more tedious task to rectify such errors than to identify and correct errors that arise in theoretical analyses.

ii. It is very difficult, sometimes impossible, to offer physical explanations of certain behaviors with numerical results.

The preceding comments are not meant to discourage a numerical approach for solving antenna problems, but rather to offer some suggestions that minimize the shortcomings of numerical methods. As a matter of fact, theoretical and numerical analysts can derive mutual benefits from each other. This may be accomplished in the following manner.

i. When a problem is solved by theoretical analysis, whether it is done rigorously or approximately, the results should be reproduced numerically. In this way confidence in the numerical method can be developed.

ii. Suppose the theoretical work is done approximately and the numerical computations are based on an exact formulation of some problem. The prominent behaviors of the theoretical analysis should also appear in the corresponding numerical results, and identification of these behaviors should be used to guide the numerical analysts in interpreting their more accurate results. If such common characteristics can be identified, the confidence in numerical results will definitely be enhanced, and thus new physical explanations might be obtained.

The numerical approaches of solving problems can be applied to antenna configurations, such as flared notches, tapered slots, finite arrays, etc.

## 13.0 CONCLUSIONS AND RECOMMENDATIONS

The preceding discussion is an attempt to explain why certain radiators are wideband. Such information is rarely found collected in one source. Some of the explanations have been gathered from sources scattered throughout the literature, and some reflect the view of the author. We cannot, however, claim that the explanations and discussions presented here are exclusive. We feel that more analytical, numerical, and experimental investigations on the subject are needed before any claim of exclusivity can be made. It has been observed, however, that if a radiator can be made to eliminate reflections somehow, it becomes broadband in general. We may call such a device reflectionless antenna (or radiator). For these reflectionless antennas, in addition to the elimination of the discontinuities other than the feed point, a matched input condition is needed.

We found that the effects of discontinuities in any antenna (dipoles and others) can be reduced to some extent by loading the radiator in question. In this manner, the loaded radiator can be transformed into a broadband antenna. Since a resistively loaded antenna suffers from inefficiency, the performance of reactively loaded antennas should be investigated both analytically and experimentally, because they are intrinsically lossless. According to Hallén [8], a capacitively loaded dipole was matched between the antenna and free space for a wide frequency range. In theoretical analyses (for both resistively and capacitively loaded antennas), one assumes continuously variable loading. However, in practice it is done in a discrete manner, so that reflections from the resulting discontinuities are small.

Although the geometries of flared and notch radiators, which gained recognition as wideband antennas, were chosen originally for the express purpose of having an antenna configuration that is reflectionless, nature apparently did not permit such perfection. We feel that an understanding of an antenna's shape is essential to characterizations of general UWB antennas and that such knowledge can be attained by considering flared antennas. To provide a basic theoretical foundation for flared notches, simpler wire antennas like the *V* and other simple shapes should be investigated in conjunction with numerical approaches to the flared notch. In particular, the author believes that numerical methods complement theoretical analyses and should not be used in the absence of theoretical work, because such an approach too often yields misleading or erroneous results. Moreover, we strongly urge the continued development of Schelkunoff's method and its application to arbitrary flared radiating structures. As noted above, these antennas are not dispersion free. To test the degree to which they are dispersive, an experiment using short pulses may help in bringing the truth to the light.

One may recall that in the frequency domain, if the input impedance (hence VSWR) and the radiation pattern of an antenna remain practically constant over a wide range (say an octave or above) of frequencies, the antenna is called broadband (or wideband). In spite of this desirable behavior, such an antenna when excited by a short pulse may radiate the same pulse with distortion. This may happen due to a shift of the phase center of the antenna with frequency. Reduction of this defect of antennas belonging to this category is suggested in the next paragraph.

For the helical and frequency-independent antenna family (log-periodic, spirals, etc.), one should make an effort to ascertain whether their performances, when subjected to a short-pulse, can be improved by employing a technique similar to the one implemented by Yatskevich et al. [45]. We also recommend conducting experiments using "lossy and tapered metalized mylar strips" on such antennas and exciting them with short-pulse inputs. Such strips may reduce the distortion due to changing phase center to a certain degree.

Fat antennas are found to be wideband. The reason may be that a fat antenna has more resonance frequencies than its thin counterpart. An area that deserves more attention than previously given is the resonance behavior of such an antenna when it is excited by short pulses. It should be pointed out, however, that fat antennas are only moderately wideband when compared with reflectionless antennas.

Wide-angle bicones have been analyzed in some detail. Not only are they UWB, but the direction of maximum radiation is frequency dependent. For example, a wide-angle bicone with equal vertex angles and the same axis of symmetry has a mainbeam that starts at broadside and approaches the cone's surface as the component frequency of the signal's spectrum increases. Since asymmetrical bicones do not radiate axially symmetrical waves, they may be relevant for radar applications. Consequently, some appropriately chosen asymmetrical bicones should be analyzed. Since the methodology for investigating symmetrical bicones is fundamental to studying asymmetrical bicones, our preliminary analysis on symmetrical bicones should be completed. Because the analysis of an asymmetrical bicone is very difficult to handle as a boundary value problem, it is not clear whether asymmetrical bicones will be more or less wideband than symmetrical ones. Before embarking on such ambitious problems, it would be both beneficial and prudent to investigate asymmetrically oriented (with respect to flat reflectors) *V*-antennas that are excited by short pulses. The results could then be used as a guide for the study of asymmetrical bicones.

Because of the apparent success of IRAs, we recommend that some time be spent on understanding their performances and analytical behavior. The numerical methods complement theoretical analysis and should be applied to flared notches and tapered slots having different analytical shapes.

Finally, we end on a philosophical note. Currently, as a result of the power of today's computers, there is a propensity for addressing radiation problems from a computational standpoint, because "results" are obtained more quickly and easily than with theoretical methods. The "results" often look good; but without corroborating analytical results, the validity of numerical "results" is in question, and a physical understanding of them is too often lacking. As a consequence, erroneous and misleading conclusions might be drawn. Numerical and experimental methods complement theoretical methods and vice versa. The point is that theoretical analyses are important and should be used in conjunction with numerical and experimental methods. Another conclusion that emerged from this study is that an UWB antenna may be characterized by its response to a short pulse. In conclusion, whatever antenna is investigated, one's approach should incorporate (1) the philosophical maxim, "the proof of an UWB antenna is in its short-pulse behavior," and (2) a synergistic merging of theoretical, numerical, and experimental methods.

## 13.0 ACKNOWLEDGEMENT

Dr. Eric Mokole provided some numerical results which were helpful in interpreting behaviors of the radiation patterns of very short as well as very long bicones. He also kindly provided a critical review of this report.

## 14.0 REFERENCES

1. W.L. Stutzman and G.A. Thiele, *Antenna Theory and Design*, pp. 239, 260-261, J. Wiley & Sons Inc, New York, NY. 1981.

2. E.C. Jordan and K.G. Balmain, *Electromagnetic Waves and Radiating System* (2nd Ed), p. 602. Prentice-Hall,Inc, Englewood Cliffs, NJ. 1968.

3. OSD/DARPA Ultra-Wideband Radar Review Panel, "Assessment of Ultra-Wideband (UWB) Technology, pp II-1-3 Report R-6280, BATTELLE Tactical Technology Center; 505 Kin Avenue, Columbus, OH 43201-2693, contract No. DAAH01-88-C-0131, ARPA order 60-49, July 13, 1990.

4. B. Noel (Ed), *Ultra-Wideband Radar: Proceedings of the First Los Alamos Symposium*, p. 463-464, CRC Press, Boca Raton, FL, 1991.

5. J.D. Taylor (Ed), *Introduction to Ultra-Wideband Radar System*, pp. 2-3, 12, 239-240, CRC Press, Inc, 1995.

6. S.N. Samaddar, "Transient radiation of single-cycle sinusoidal pulse from a thin dipole," *J. Franklin Inst.*, Vol. 329, No. 2, pp. 259-271, 1992.

7. S.N. Samaddar, "Behavior of a received pulse radiated by a half-wave dipole excited by a single-cycle sinusoidal voltage," *J. Franklin Inst.*, Vol. 330, No. 1, pp. 17-28, 1993.

8. E. Hallén, *Electromagnetic Theory*, 501-502, J. Wiley & Sons Inc, New York, NY. 1962.

9. T.T. Wu and R.W.P. King, "The cylindrical antenna with non-reflecting resistive loading," *IEEE Trans Antennas Propagat.*, Vol. 13, pp. 369-373, May 1965. Correction, p. 998, Nov 1965.

10. L.C. Shen and T.T. Wu, "Cylindrical antenna with tapered resistive loading," *Radio Sci.*, Vol. 2, pp. 191-205, Feb 1967.

11. J.B.L. Rao, J.E. Ferris and W.E. Zimmerman, "Broadband characteristics of cylindrical Antennas with exponentially tapered capacitive loading," *IEEE Trans. Antennas Propagat.*, Vol AP-17, pp. 145-151, March 1969.

12. J.G. Maloney and G.S. Smith, "A study of transient radiation from the Wu-King resistive monopole - FDTD analysis and experimental measurements," *IEEE Trans. Antennas Propagat.*, Vol 41, pp. 668-676, May 1993.

13. J. G. Maloney and G.S. Smith, "Optimization of a conical antenna for pulse radiation: an efficient design using resistive loading," *IEEE Trans. Antennas Propagat.*, Vol 41, pp. 940-947, July 1993.

14. M. Parent, private communication, March 1995.

15. J.D. Kraus, *Antennas* (2nd ed.), McGraw-Hill Company, New York, NY, 1988.

16. D.L. Sengupta and J.E. Ferris, "Investigation of the rudimentary horn (Final Report)," AD857364, The University of Michigan, E.E. Dept., Radiation Laboratory, Ann Arbor, MI, May 1969.

17. S.A. Schelkunoff, "Conversion of Maxwell's equations into generalized telegraphist's equations,", *Bell System Technical Journal*, pp. 995-1043, 1955.

18. T.S.M Maclean, *Principles of Antennas: Wire and Aperture*, Cambridge University Press, Cambridge, England, 1986.

19. J.S. Chatterjee, "Radiation field of a conical helix," *J. Appl. Phys*, Vol. 24, No. 5, pp. 550-559, 1953.

20. J.S. Chatterjee, "Radiation characteristics of a conical helix of low pitch angle," *J. Appl. Phys*, Vol. 26, No. 3, pp. 331-335, 1954.

21. E.T. Kornhauser, "Radiation field of helical antennas with sinusoidal current," *J. Appl Phys*, Vol. 22, No. 7, pp. 887-891, 1951.

22. V.H. Rumsey, *Frequency Independent Antennas*, Academic Press, 1966.

23. J.D. Dyson, "Equiangular spiral antennas," *IRE Trans. Antennas Propagat.*, AP-7, pp. 181-187, 1959.

24. R.S. Elliott, "A view of frequency independent antennas," *The Microwave Journal*, pp. 61-68, December 1962.

25. L.J. Chu and J.A. Stratton, "Steady-state solutions of electromagnetic field problems. Forced oscillations of a conducting sphere," *J. Appl Phys*, Vol. 12, No. 12, pp. 236-240, March 1941.

26. L.J. Chu and J.A. Stratton, "Steady-state solutions of electromagnetic field problems. Forced oscillations of a prolate spheroid," *J. Appl Phys*, Vol. 12, No. 12, pp. 241-248, 1941.

27. G. Franceschetti, "A cononical problem in transient radiation - the spherical antenna," *IEEE Trans. Antennas Propagat.*, AP-26, pp. 551-555, July 1978.

28. O.M. Bucci and G. Franceschetti, "Input admittance and transient response of spheroidal antennas in dispersive media," *IEEE Trans. Antennas Propagat.*, AP-22, pp. 526-536, July 1974.

29. V.A. Fok, *Electromagnetic Diffraction and Propagation,* Pergamon Press, New York, 1965.

30. S.A. Schelkunoff, *Electromagnetic Waves,* Van Nostrand, 1948.

31. P.D. P. Smith, "The conical dipole of wide-angle," *J. Appl. Phys,* Vol. 19, pp. 11-23, 1948.

32. C.T. Tai, "On the theory of biconical antennas," *J. Appl. Phys,* Vol. 19, pp. 1155-1160, 1948.

33. C.T. Tai, "A study of the E.M.F. method," *J. Appl. Phys,* Vol. 20, pp. 717-723, 1949.

34. C.T. Tai, "Application of variational principle to biconical antennas," *J. Appl. Phys,* Vol. 20, pp. 1076-1048, 1949.

35. C.H. Papas and R.W.P. King, "Input impedance of wide-angle conical antennas fed by a coaxial line," *Proc. IRE,* Vol. 37, pp. 1269-1271, 1949.

36. C.H. Papas and R.W.P. King, "Radiation from wide-angle conical antennas fed by a coaxial line," *Proc. IRE,* Vol. 39, pp. 49-51, 1951.

37. S.S. Sandler and R.W.P. King "Compact conical antennas for wide-band coverage," *IEEE Trans. Antennas Propagat.*, Vol. AP-42, pp. 436-439, 1994.

38. C.W. Harrison and C.S Williams, "Transients in wide-angle conical antennas," *IEEE Trans. Antennas Propagat.*, AP-13, pp. 230-246, 1965.

39. C.E. Baum and E.G. Farr, "Impulse radiating antennas," in *Ultra-Wideband Short-Pulse Electromagnetics, ed. H. Bertoni et al., Plenum Press*, pp. 139 and 147, 1993.

40. R.L. Carrel, "The characteristic impedance of two infinite cones of arbitrary cross-section," *IEEE Trans. Antennas Propagat.*, AP-6, pp. 197-201, 1958.

41. H.M. Shen, R.W.P. King and T.T. Wu, "V-conical antenna," *IEEE Trans. Antennas Propagat.*, AP-36, pp. 1519-1525, 1988.

42. R. Janaswamy, D.H. Schaubert and D.M. Pozar, "Analysis of the transverse electromagnetic mode linearly tapered slot antennas," *Radio Sci.*, Vol. 21, pp. 797-804, September-October 1986.

43. H.F. Harmuth, "Radiation of Nonsinusoidal Electromagnetic Waves," Academic Press, 1990.

44. H.F. Harmuth, "Antennas and waveguides for Nonsinusoidal Waves," Academic Press, 1984.

45. V.A. Yatskevich and L.L. Fedosenko, "Antennas for radiation of very-wide-band signal," *Izvestiya Vuz. Radioelektronika,* Vol. 29, No. 2, pp. 69-74, 1986.

46. A. Erdélyi and Staff of the Harry Bateman Manuscript Project, *Higher Transcendental Functions, Vol. 2,* Eq. 53, p. 183, McGraw-Hill, New York, 1953.

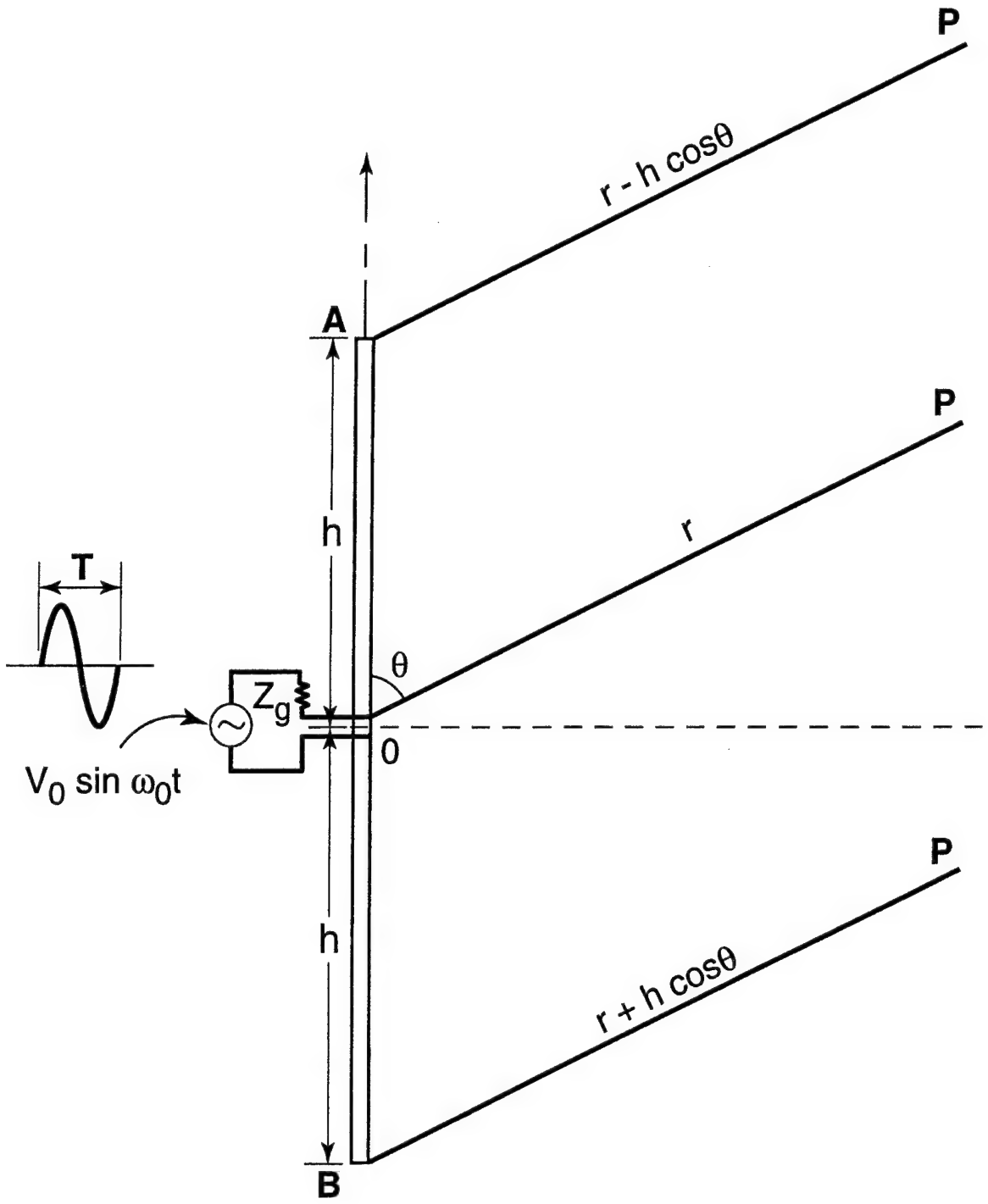


Fig. 1 - Transient Radiation from a Vertical Dipole Antenna Oriented Along the z-axis

## Appendix A

## BICONICAL ANTENNAS WITH UNEQUAL CONE ANGLES

### SUMMARY

Here we generalize the biconical antenna analyses previously provided by Schelkunoff [30], Smith [31], and Tai [32-34] by considering axially symmetric bicones having unequal half-cone angles $\psi_1$ and $\psi_2$, respectively. The bicones are excited symmetrically at the apices by a voltage source so that higher order modes consist of TM only. Formal expressions for the field components are presented in each regions. A variational expression for the terminal admittance is derived. Wide-angle approximations are also made so that the higher order TM modes in the antenna region ($0 \leq r \leq a$) can be neglected, $a$ being the length of each cone. Effective length of the biconical antenna for the far field is also presented. The concept of the effective length is useful when the antenna is used for reception. Limiting values (for small cones $ka << 1$ as well as very large cones $ka >> 1$) of some parameters, such as effective length, radiated field, etc. are discussed. It has been shown that the radiation pattern of a very small cone is proportional to sin $\theta$ (similar to that of a dipole), whereas it behaves like 1/sin $\theta$ for a large cone (i.e. $ka >> 1$). In this way we have also generalized the theoretical results of some of the previous authors [30-38]. Although most of the analyses are presented in the frequency domain, transient response of such antennas are discussed in some special cases, similar to the situations presented by Harrison and Williams [38].

### INTRODUCTION

The geometry of the antenna configuration is shown in Fig. 1. The common axis of the two cones is oriented along the $z$-axis, with which the cones make angles $\psi_1$ and $\psi_2$, respectively. The bicones are excited at the apices symmetrically by a voltage source, so that only TEM and TM modes are generated. The field components can then be expressed in term of a scalar function $\Pi(r,\theta)$, which becomes equivalent to the radial component of the vector potential. The spherical coordinates $(r,\theta)$ are referred to the origin at the apices of the cones. Suppressing the assumed time dependence exp $(i\omega t)$, the field components can be expressed as follows.

$$rH_\phi = -\frac{\partial}{\partial\theta}\,\Pi(r,\theta), \tag{1a}$$

$$rE_r = \frac{r}{i\omega\epsilon_0}\left[\frac{\partial^2}{\partial r^2} + k^2\right]\Pi(r,\theta) = \frac{\nu(\nu+1)}{i\omega\epsilon_0 r}\,\Pi(r,\theta), \tag{1b}$$

$$rE_\theta = \frac{1}{i\omega\epsilon_0}\,\frac{\partial^2}{\partial r\partial\theta}\,\Pi(r,\theta), \tag{1c}$$

where $k = \omega\sqrt{\mu_0\epsilon_0}$ . The components $E_r$ and $E_\theta$ can also be expressed in terms of $H_\phi$ in the following way.

$$rE_\theta = -\frac{1}{i\omega\epsilon_0}\frac{\partial}{\partial r}(rH_\phi), \tag{2a}$$

$$rE_r = \frac{1}{i\omega\epsilon_0 r \sin\theta}\frac{\partial}{\partial\theta}[\sin\theta(rH_\phi)]. \tag{2b}$$

The boundary conditions to be satisfied by the field components are:

$$\left.\begin{aligned} &E_r(r,\psi_1) = 0 \quad , \quad 0 < r \le a \\ &E_r(r,\pi - \psi_2) = 0 \end{aligned}\right\} \tag{3a}$$

$rH_\phi(r,\theta)$ is continuous at $r = a$, for $\psi_1 \le \theta \le \pi - \psi_2$, (3b)

$E_r(r,\theta)$ is continuous at $r = a$, for $\psi_1 < \theta < \pi - \psi_2$, (3c)

$rE_\theta$ is continuous at $r = a$, for $\psi_1 < \theta < \pi - \psi_2$. (3d)

In addition $E_\theta$ on the metallic spherical caps of the cones at $r = a$ must vanish. All the field components in the region $r > a$ are outgoing waves.

**ANALYSIS**

The formal expressions of the field components in various regions are presented in the following.

$$i\omega\epsilon_0 r^2 E_r = -\sum_{\nu_p} \frac{a_{\nu_p}}{2\pi}\frac{S_{\nu_p}(kr)}{S_{\nu_p}(ka)} T_{\nu_p}(\theta) \quad , \quad 0 < r < a, \tag{4a}$$

$$\left.\begin{aligned} rE_\theta = {} & \frac{I_0 Z_0}{2\pi \sin\theta}\left[(1 + Z_c Y_t)e^{-ik(r-a)} + (1 - Z_c Y_t)e^{ik(r-a)}\right] \\ & -iZ_0 \sum_{\nu_p} \frac{a_{\nu_p}}{2\pi\nu_p(\nu_p + 1)}\frac{S'_{\nu_p}(kr)}{S_{\nu_p}(ka)}\frac{\partial}{\partial\theta} T_{\nu_p}(\theta) \quad , \quad 0 < r \; a \end{aligned}\right\} \tag{4b}$$

$$\left.\begin{aligned} rH_\phi = {} & \frac{I_0}{2\pi \sin\theta}\left[(1 + Z_c Y_t)e^{-ik(r-a)} - (1 - Z_c Y_t)e^{ik(r-a)}\right] \\ & -\sum_{\nu_p} \frac{a_{\nu_p}}{2\pi\nu_p(\nu_p + 1)}\frac{S_{\nu_p}(kr)}{S_{\nu_p}(ka)}\frac{\partial}{\partial\theta} T_{\nu_p}(\theta) \quad , \quad 0 < r < a \end{aligned}\right\} \tag{4c}$$

where $Z_0 = \sqrt{\mu_0/\epsilon_0} = 120\,\pi$, $Z_c$, the characteristic impedance of the bicone is given by [30]

$$\begin{aligned} Z_c &= \frac{Z_0}{2\pi}\int_{\psi_1}^{\pi-\psi_2}\frac{d\theta}{\sin\theta} = \frac{Z_0}{2\pi}\ln[\cot(\psi_1/2)\cot(\psi_2/2)] \\ &= Z_c(\psi_1,\psi_2). \end{aligned} \tag{5a}$$

$$T_{\nu_p}(\theta) = P_{\nu_p}(\cos\theta)P_{\nu_p}(-\cos\psi_1) - P_{\nu_p}(-\cos\theta)P_{\nu_p}(\cos\psi_1), \tag{5b}$$

where $P_{\nu_p}(\cos\theta)$ is a Legendre function and $\nu_p$ which are non-integers in general are the solution of

$$T_{\nu_p}(\pi - \psi_2) = P_{\nu_p}(-\cos\psi_2)P_{\nu_p}(-\cos\psi_1) - P_{\nu_p}(-\cos\psi_2)P_{\nu_p}(\cos\psi_1) = 0, \tag{5c}$$

with $p = 1, 2, \ldots$ . Equations (5b) and (5c) satisfy the boundary condition that $E_r$ vanishes on the surfaces of the cones for $0 < r < a$.

$$S_{\nu_p}(kr) = \sqrt{kr}\; J_{\nu_p+1/2}(kr) \text{ and } S'_{\nu_p}(kr) = \frac{d}{d(kr)} S_{\nu_p}(kr). \tag{5d}$$

The function $Y_t$ represents the terminal admittance (at $r = a$) of the biconical antenna.

Outside the antenna region ($r > a$) we have

$$i\omega\epsilon_0 r^2 E_r = -\sum_{t=1}^{\infty} \frac{b_t}{2\pi} \frac{R_t(kr)}{R_t(ka)} P_t(\cos\theta),\ r > a, \tag{6a}$$

$$rE_\theta = -iZ_0 \sum_{t=1}^{\infty} \frac{b_t}{2\pi\ell(\ell+1)} \frac{R'_t(kr)}{R_t(ka)} \frac{\partial}{\partial\theta} P_t(\cos\theta), r > a, \tag{6b}$$

$$rH_\phi = -\sum_{t=1}^{\infty} \frac{b_t}{2\pi\ell(\ell+1)} \frac{R_t(kr)}{R_t(ka)} \frac{\partial}{\partial\theta} P_t(\cos\theta),\ r > a, \tag{6c}$$

where

$$R_t(kr) = \sqrt{kr}\; H^{(2)}_{t+1/2}(kr) \text{ and } R'_t(kr) = \frac{d}{d(kr)} R_n(kr). \tag{6d}$$

Since $\ell$ is an integer $P_t(\cos\theta)$ is a Legendre polynomial.

It can be shown that

$$I_0 = \frac{a}{2Z_c} \int_{\psi_1}^{\pi-\psi_2} E_\theta(a,\theta)d\theta. \tag{7}$$

**DETERMINATION OF $a_{\nu_p}$, $b_t$ and $Y_t$**

Since $E_r$ is continuous at $r = a$ for $\psi_1 < \theta < \pi - \psi_2$, one finds from (4a) and (6a) the following relation.

$$\sum_t b_t P_t(\cos\theta) = \sum_{\nu_p} a_{\nu_p} T_{\nu_p}(\theta) \quad , \quad \psi_1 < \theta < \pi - \psi_2. \tag{8}$$

Equating (4c) and (6c) at $r = a$ for $\psi_1 \le \theta \le \pi - \psi_2$, we have

$$\left.\begin{aligned} \frac{2I_0Z_cY_t}{\sin\theta} - \sum_{\nu_p} \frac{a_{\nu_p}}{\nu_p(\nu_p+1)} \frac{\partial}{\partial\theta} T_{\nu_p}(\theta) \\ = -\sum_{t=1} \frac{b_t}{t(t+1)} \frac{\partial}{\partial\theta} P_t(\cos\theta). \end{aligned}\right\} \tag{9}$$

Integrating both sides of (9) with respect to $\theta$ from $\theta = \psi_1$ to $\theta = \pi - \psi_2$, one finds after using the boundary conditions

$$Y_t = \left[\frac{Z_0}{2\pi Z_c}\right]^2 \sum_{t=1}^{\infty} \frac{\hat{b}_t}{t(t+1)} [P_t(\cos\psi_1) - (-1)^t P_t(\cos\psi_2)], \tag{10a}$$

where

$$\hat{b}_t = b_t\pi/(Z_0 I_0). \tag{10b}$$

When $\psi_1 = \psi_2 = \psi$, the relation (10a) reduces to Eq. (14) of Tai [32], i.e.,

$$Y_t = \left[\frac{Z_0}{2\pi Z_c}\right]^2 \sum_{t=1,3,5,\ldots} \frac{2\hat{b}_t}{t(t+1)} P_t(\cos\psi). \tag{10c}$$

Equating (4b) and (4c) at $r = a$ one obtains the following relations

$$-\frac{iZ_0}{2\pi a} \sum_{t=1} \frac{b_t}{t(t+1)} M_t \frac{\partial}{\partial\theta} P_t(\cos\theta) = \begin{cases} E_a(\theta), & \psi_1 \le \theta \le \pi - \psi_2 \\ 0, & \begin{cases} 0 \le \theta \le \psi_1 \\ \pi - \psi_2 \le \theta \le \pi \end{cases} \end{cases} \tag{11a}$$

where

$$E_a(\theta) \equiv E_\theta(a,\theta) = \frac{I_0Z_0}{\pi a \sin\theta} - \frac{iZ_0}{2\pi a} \sum_{\nu_p} \frac{a_{\nu_p}}{\nu_p(\nu_p+1)} N_{\nu_p} \frac{\partial}{\partial\theta} T_{\nu_p}(\theta) \qquad \psi_1 \le \theta \le \pi - \psi_2 \tag{11b}$$

where

$$M_t = R_t'(ka)/R_t(ka), \tag{12a}$$

$$N_{\nu_p} = S_{\nu_p}'(ka)/S_{\nu_p}(ka). \tag{12b}$$

Noting that over the spherical cap of the metallic cones $E_\theta$ vanishes, we multiply (11a) and (11b) by $\sin\theta \frac{\partial P_r}{\partial\theta}(\cos\theta)d\theta$, $r$ being integers, and then integrating $\theta = 0$ to $\pi$, we have

$$[P_r(\mu_1) - (1)^r P_r(\mu_2)] = -iZ_0 \sum_{\nu_p} \frac{\hat{a}_{\nu_p}(r+1)rN_{\nu_p}}{\pi\nu_p(\nu_p+1)} I_{\nu_p,r} + \frac{iZ_0\hat{b}_r M_r}{\pi(2r+1)\Omega(\psi_2)} \Bigg\} \tag{13}$$

where $\mu_1 = \cos\psi_1$, $\mu_2 = \cos\psi_2$ and

$$I_{\nu_p,r} = \frac{\left[(1-\mu_1^2)P_r(\mu_1)\frac{\partial}{\partial\mu}T_{\nu_p}(\mu)\Big|_{\mu=\mu_1} - (-1)^r(1-\mu_2^2)P_r(\mu_2)\frac{\partial}{\partial\mu}T_{\nu_p}(\mu)\Big|_{\mu=-\mu_2}\right]}{[r(r+1)-\nu_p(\nu_p+1)]}, \tag{14a}$$

$$= \int_{-\mu_2}^{\mu_1} T_{\nu_p}(\mu)P_r(\mu)d\mu, \tag{14b}$$

$$\Omega(\psi_2) = 1 + \delta_{\psi_2,\pi/2} = \begin{cases} 1, & \psi_2 \neq \pi/2 \neq \psi_1 \\ 2, & \psi_2 = \pi/2 \neq \psi_1 \end{cases}. \tag{14c}$$

Here we have introduced the function $\Omega(\psi_2)$ to take into account of the situation when the cone with angle $\psi_2$ is replaced by an infinite perfect conductor at the plane $z = 0$, Fig. 2 [such as in Ref. 35-38]. Now from (8) we have, after noting that $T_{\nu_p}(\theta)$ is orthogonal in the range $\psi_1 \le \theta \le \pi - \psi_2$, the following expression

$$a_{\nu_p} = \sum_{t=1}^{\infty} b_t[I_{\nu_p,t} / \hat{I}_{\nu_p,\nu_p}], \tag{15a}$$

where $\hat{I}_{\nu_p,\nu_p}$ is given by

$$\hat{I}_{\nu_p,\nu_p} = \int_{-\mu_2}^{\mu_1}[T_{\nu_p}(\mu)]^2 d\mu = \left[(1-\mu_1^2)\left[\frac{\partial T_{\nu_p}(\mu)}{\partial\nu_p}\right]_{\mu=\mu_1}\right.$$

$$\left. \cdot \left[\frac{\partial}{\partial\mu}T_{\nu_p}(\mu)\right]_{\mu=\mu_1} - (1-\mu_2^2)\left[\frac{\partial T_{\nu_p}(\mu)}{\partial\nu_p}\right]_{\mu=-\mu_2} \cdot \left[\frac{\partial T_{\nu_p}(\mu)}{\partial\mu}\right]_{\mu=-\mu_2}\right] \Big/ (2\nu_p+1). \tag{15b}$$

Substituting (16a) for $a_{\nu_p}$ in (13) one finds

$$[P_r(\mu_1) - (-1)^r P_r(\mu_2)] = \frac{ib_r M_r}{\Omega(\psi_2)I_0(2r+1)} - \frac{ir(r+1)}{2I_0}\sum_{\nu_p}\sum_{t=1}\frac{N_{\nu_p}b_t I_{\nu_p,r}I_{\nu_p,t}}{\nu_p(\nu_p+1)\hat{I}_{\nu_p,\nu_p}}. \tag{16}$$

Replacing $[P_\mu(\mu_1) - (-1)^r P_r(\mu_2)]$ in (10b) by the right-hand side of (16), we have expression for the terminal admittance $Y_t$

$$Y_t = \frac{iZ_0}{4\pi I_0^2 Z_c^2}\left[\sum_{r=1}\frac{b_r^2 M_r}{\Omega(\psi_2)r(r+1)(2r+1)} - \sum_{\nu_p}\sum_{r=1}\sum_{t=1}\frac{b_r b_t N_{\nu_p}}{2\nu_p(\nu_p+1)}\frac{I_{\nu_p,r}I_{\nu_p,t}}{\hat{I}_{\nu_p,\nu_p}}\right]. \tag{17}$$

When TM waves or complementary waves in the antenna region (i.e., $0 \le r \le a$) are negligible, then $\hat{a}_{\nu_r}$ in (13) can be neglected. This assumption appears to be accurate for wide-angle cones. Thus from (13) we have the following approximate value of $\hat{b}_r$

$$\hat{b}_r \simeq \frac{-i\pi(2r+1)}{Z_0 M_r} [P_r(\mu_1) - (-1)^r P_r(\mu_2)]\Omega(\psi_2). \tag{18}$$

Subject to this condition (which may be called the zero-order approximation) the expression for the terminal admittance becomes

$$Y_{t0} = \frac{-iZ_0}{4\pi Z_c^2} \sum_{r=1}^{\infty} \frac{(2r+1)\Omega(\psi_2)}{r(r+1)M_r} [P_r(\mu_1) - (-1)^r P_r(\mu_2)]^2. \tag{19}$$

The expression (19) can also be obtained from (17) by neglecting the series consisting of triple sum and then replacing $\hat{b}_r$ by (18) with the aid of (10b).

## A VARIATIONAL EXPRESSION FOR THE TERMINAL ADMITTANCE $Y_t$

With the aid of (11a) and (11b) $b_r$ and $a_{\nu_r}$ can also be expressed as follows in terms of the aperture electric field $E_a(\theta)$ at $r = a$.

$$b_r = \frac{i2\pi a\Omega(\psi_2)}{Z_0 M_r I_{r,r}} \int_{\psi_1}^{\pi-\psi_2} E_a(\theta) \frac{\partial}{\partial\theta} P_r(\theta) \sin\theta \, d\theta, \tag{20a}$$

where $$I_{r,r} = \int_0^{\pi} [P_r(\cos\theta)]^2 \sin\theta \, d\theta = \frac{2}{2r+1}, \tag{20b}$$

$$a_{\nu_r} = \frac{i2\pi a}{Z_0 N_{\nu_r} \hat{I}_{\nu_r,\nu_r}} \int_{\psi_1}^{\pi-\psi_2} E_a(\theta) \sin\theta \frac{\partial}{\partial\theta} T_{\nu_r}(\theta) d\theta. \tag{20c}$$

Substituting now (7), (20a) and (20c) for $I_0$, $b_r$ and $a_{\nu_r}$, respectively, in the expression (9), we have

$$[Y_t/(2\pi \sin\theta)] \left\{ \int_{\psi_1}^{\pi-\psi_2} E_a(\theta') d\theta' \right\}$$

$$- (i/Z_0) \sum_{\nu_r} \frac{\frac{\partial}{\partial\theta} T_{\nu_r}(\theta)}{\nu_p(\nu_p+1) N_{\nu_r} \hat{I}_{\nu_r,\nu_r}} \left\{ \int_{\psi_1}^{\pi-\psi_2} E_a(\theta') \sin\theta' \frac{\partial}{\partial\theta'} T_{\nu_r}(\theta') d\theta' \right\}$$

$$= (-i/Z_0) \sum_{r=1} \frac{\Omega(\psi_2) \frac{\partial}{\partial\theta} P_r(\cos\theta)}{r(r+1)M_R I_{r,r}} \left\{ \int_{\psi_1}^{\pi-\psi_2} E_a(\theta') \sin\theta' \frac{\partial}{\partial\theta'} P_r(\cos\theta') d\theta' \right\}. \tag{21}$$

Equation (21) is the integral equation for the unknown aperture field $E_a(\theta)$. First multiplying both sides of (21) by $E_a(\theta) \sin\theta \, d\theta$ and then integrating from $\theta = \psi_1$ to $\pi - \psi_2$ we have the following expression for $Y_t$

$$Y_t = \frac{i2\pi}{Z_o}\left[\int_{\psi_1}^{\pi-\psi_2} E_a(\theta)d\theta\right]^{-2}\cdot\left[\sum_{\nu_p}[\nu_p(\nu_p+1)N_{\nu_p}\hat{I}_{\nu_p,\nu_p}]^{-1}\cdot\left\{\int_{\psi_1}^{\pi-\psi_2} E_a(\theta)\sin\theta\,\frac{\partial}{\partial\theta}T_{\nu_p}(\theta)d\theta\right\}^2\right.$$

$$\left.-\sum_{r=1}\Omega(\psi_2)[r(r+1)M_rI_{r,r}]^{-1}\cdot\left\{\int_{\psi_1}^{\pi-\psi_2} E_a(\theta)\sin\theta\,\frac{\partial}{\partial\theta}P_t(\cos\theta)d\theta\right\}^2\right]. \tag{22}$$

It can be shown that $Y_t$, given by (22) is in a variational form with respect to the variation of the aperture field $E_a(\theta)$.

## EVALUATION OF $Y_t$

Let us expand the aperture field $E_a(\theta)$ in the following form

$$E_a(\theta) = -\frac{A_0}{\sin\theta} + \sum_{\nu_m} A_{\nu_m}\frac{\partial}{\partial\theta}T_{\nu_m}(\theta). \tag{23}$$

This form of representation for $E_a(\theta)$ is implied by (11b). Since $E_a(\theta)$ appears in both the numerator and the denominator of the right-hand side of (22), we may normalize $A_0$ by unity. Then carrying out the integrals in (22) using (23), $Y_t$ can be expressed as follows.

$$Y_t = \frac{iZ_0}{2\pi Z_c^2}\left[-\sum_{s=1}^{\infty}\Omega(\psi_2)\frac{\{P_s(\mu_1)-(-1)^sP_s(\mu_2)\}^2}{s(s+1)M_sI_{s,s}} + \sum_{\nu_p}\nu_p(\nu_p+1)\hat{I}_{\nu_p,\nu_p}A_{\nu_p}^2/N_{\nu_p}\right.$$

$$-\sum_{s=1}^{\infty}\sum_{\nu_m}\Omega(\psi_2)2\{P_s(\mu_1)-(-1)^sP_s(\mu_2)\}I_{\nu_m,t}A_{\nu_m}/(M_sI_{s,s}) \tag{24}$$

$$\left.-\sum_{s=1}^{\infty}\sum_{\nu_m}\sum_{\nu_n}\Omega(\psi_2)s(s+1)I_{\nu_m,s}I_{\nu_n,s}A_{\nu_m}A_{\nu_n}/(M_sI_{s,s})\right].$$

In order to simplify (24) let us introduce $\beta_{\nu_m}$, $\alpha_{\nu_m}$ and $\gamma_{\nu_m,\nu_n} = \gamma_{\nu_n,\nu_m}$ as follows

$$\beta_{\nu_m} = [iZ_0/(2\pi Z_c^2)]\cdot[\nu_m(\nu_m+1)\hat{I}_{\nu_m,\nu_m}/N_{\nu_m}], \tag{25a}$$

$$\alpha_{\nu_m} = [-iZ_0/(\pi Z_c^2)]\sum_{s=1}\Omega(\psi_2)[P_s(\mu_1)-(-1)^sP_s(\mu_2)]I_{\nu_m,s}/(2I_{s,s}M_s), \tag{25b}$$

$$\gamma_{\nu_n,\nu_m} = \gamma_{\nu_m,\nu_n} = [-iZ_0/(2\pi Z_c^2)]\sum_{s=1}^{\infty}\Omega(\psi_2)s(s+1)I_{\nu_n,s}I_{\nu_m,s}/(M_sI_{s,s}). \tag{25c}$$

With the aid of (19) and (25a) to (25c), the representation for $Y_t$ given by (24) can be cast into the following form

$$Y_t = Y_{t0} + \sum_{\nu_n}\beta_{\nu_n}A_{\nu_n}^2 + 2\sum_{\nu_n}\alpha_{\nu_n}A_{\nu_n} + \sum_{\nu_m}\sum_{\nu_n}\gamma_{\nu_m}\gamma_{\nu_n}A_{\nu_m}A_{\nu_n}. \tag{26a}$$

Since $Y_t$ is stationary with respect to the variation of $E_a(\theta)$, we determine the unknown coefficients $A_{\nu_m}$

by letting $\frac{\partial}{\partial A_{\nu_m}} Y_t = 0$, which gives

$$\beta_{\nu_n} A_{\nu_n} + \alpha_{\nu_n} + \sum_{\nu_m} \gamma_{\nu_m \nu_n} A_{\nu_m} = 0. \tag{26b}$$

Multiplying (26b) by $A_{\nu_n}$ and then summing over $\nu_n$ we have

$$\sum_{\nu_n} \beta_{\nu_n} A_{\nu_n}^2 + \sum_{\nu_n} \alpha_{\nu_n} A_{\nu_n} + \sum_{\nu_n} \sum_{\nu_m} \gamma_{\nu_m \nu_n} A_{\nu_m} A_{\nu_n} = 0 . \tag{26c}$$

Subtracting now (26c) from (26a), we have the desired expression for $Y_t$ given by

$$Y_t = Y_{t0} + \sum_{\nu_n} \alpha_{\nu_n} A_{\nu_n} . \tag{27}$$

If the first term on the right-hand side of (27) is called "zero order solution," then the second term may be called the "correction term."

## WIDE-ANGLE APPROXIMATION

As stated earlier, in this approximation the complementary waves (TM modes) in the antenna region ($0 < r < a$) are negligible, i.e. $a_{\nu_n} \simeq 0$. Then the field components can be expressed as [for $0 < r < a$].

$$E_\theta = \frac{Z_0}{r \sin \theta} [\sigma_1 e^{-ikr} - \sigma_2 e^{ikr}] , \tag{28a}$$

$$H_\phi = \frac{1}{r \sin \theta} [\sigma_1 e^{-ikr} + \sigma_2 e^{ikr}] , \tag{28b}$$

where

$$\sigma_1 = I_0(Z_c Y_t + 1) e^{ika}/2\pi , \tag{29a}$$

$$\sigma_2 = I_0(Z_c Y_t - 1) e^{-ika}/2\pi . \tag{29b}$$

The ratio,

$$\sigma_2/\sigma_1 = e^{-i2ka}(Z_c Y_t - 1)/(Z_c Y_t + 1) \tag{29c}$$

is the reflection coefficient.

In the exterior region ($r > a$), we have

$$E_\theta = iZ_0 \sum_{n=1}^{\infty} B_n \left[ h_{n-1}^{(2)}(kr) - \frac{n}{kr} h_n^{(2)}(kr) \right] P_n^1(\cos \theta), \tag{30a}$$

and

$$H_\phi = \sum_{n=1}^{\infty} B_n h_n^{(2)}(kr) P_n^1(\cos\theta), \tag{30b}$$

where we have introduced the following relations.

$$h_n^{(2)}(x) = \sqrt{\frac{\pi}{x}}\, H_{n+1/2}^{(2)}(x), \tag{31a}$$

$$B_n = b_n/[2\pi a\, n(n+1)\, h_n^{(2)}(ka)], \tag{31b}$$

and

$$P_n^1(\cos\theta) = -\frac{\partial}{\partial\theta} P_n(\cos\theta)\ . \tag{31c}$$

It can also be shown that the input current $I(0)$ (which is not $I_0$) is given by

$$I(0) = \lim_{r\to 0} [2\pi r \sin\psi_1 H_\phi(r,\psi)] = 2\pi(\sigma_1 + \sigma_2)\ , \tag{32a}$$

and the input voltage $V(0)$ is

$$V(0) = 2\pi Z_c(\sigma_1 - \sigma_2) = \int_{\psi_2}^{\pi-\psi_2} rE_\theta(r,\theta)d\theta\ , \tag{32b}$$

$$I_0 = \pi(\sigma_1 e^{-ika} - \sigma_2 e^{ika})\ , \tag{32c}$$

$$= I(0) \,/\, [2\{Z_c Y_t \cos ka + i \sin ka\}]\ . \tag{32d}$$

The input impedance $Z_{in}$ is given by

$$Z_{in} = V(0) \,/\, I(0) = Z_c \left[\frac{\sigma_1 - \sigma_2}{\sigma_1 + \sigma_2}\right]. \tag{33}$$

Then setting $a_{\nu} = 0$ in (13) and using (31b), one can determine $B_n$ as

$$B_n = -\frac{i}{2a}\,\frac{2n+1)}{n(n+1)}\,\frac{(\sigma_1 e^{-ika} - \sigma_2 e^{ika})\,[P_n(\mu_1) - (-1)^n P_n(\mu_2)]\,\Omega(\psi_2)}{\left[h_{n-1}^{(2)}(ka) - \frac{n}{ka}\, h_n^{(2)}(ka)\right]}\ . \tag{34}$$

The substitution of $B_n$ in (30b) and (30c) gives the field components in the exterior region $r > a$. The radiated electric field $E_\theta$, for which $kr >> 1$ and

$$\text{and} \quad \left.\begin{aligned} h_n^{(2)}(kr) &\sim (i)^{n+1} e^{-ikr} \,/\, (kr) \\ h_{n-1}^{(2)}(kr) &\sim i^n e^{-ikr} \,/\, (kr) \end{aligned}\right\} \tag{35}$$

can be represented in the following manner in terms of the effective height $h_e(\theta,\omega)$.

$$E_\theta^{rad}(r,\theta,\omega) = \frac{iZ_0}{2\pi}\left[\frac{e^{-ikr}}{r}\right] I(0)\,[kh_e(\theta,\omega)], \tag{36a}$$

where

$$kh_e(\theta,\omega) = \frac{[e^{-ika} - (\sigma_2/\sigma_1)e^{ika}]}{ka(1 + \sigma_2/\sigma_1)} \sum_{n=1} \frac{i^{n-1}(2n+1)}{n(n+1)} \frac{P_n^1(\cos\theta)\, g_n(\mu_1,\mu_2)\Omega(\psi_2)}{\left[h_{n-1}^{(2)}(ka) - \frac{n}{ka} h_n^{(2)}(ka)\right]}, \tag{36b}$$

The function $g_n(\mu_1,\mu_2)$ is defined by

$$g_n(\mu_1,\mu_2) = P_n(\mu_1) - (-1)^n P_n(\mu_2) \tag{36c}$$

and $I(0)$ is given by (32a).

Equating (28b) and (30b) at $r = a$, and then integrating with respect to $\theta$ from $\theta = \psi_1$ to $\pi - \psi_2$, one finds a relation (upon using (5a), (34) and (36c)), which can be expressed as

$$[1 + (\sigma_2/\sigma_1)e^{i2ka}]/[1 - (\sigma_2/\sigma_1)e^{i2ka}] = -\frac{i\hat{S}}{4\pi(Z_c/Z_0)} = -iS\,, \tag{37a}$$

where

$$\hat{S} = \sum_{n=1}^{\infty} \frac{(2n+1)[g_n(\mu_1,\mu_2)]^2 \zeta_n(ka)\Omega(\psi_2)}{n(n+1)}\,, \tag{37b}$$

and

$$\zeta_n(ka) = h_n^{(2)}(ka) \,/\, \left[h_{n-1}^{(2)}(ka) - \frac{n}{ka} h_n^{(2)}(ka)\right]\,. \tag{37c}$$

The unknown ratio $\sigma_2/\sigma_1$ can then be calculated (from (37a)) in terms of $\hat{S}$ in the following manner

$$\sigma_2/\sigma_1 = e^{-i2ka}\,[1 + iS] \,/\, [-1 + iS]\,. \tag{38a}$$

Comparing (29c) and (38a) one finds the following expression for the terminal admittance

$$Y_{t0} = (-iS)/Z_c \tag{38b}$$

$$= [1 + (\sigma_2/\sigma_1)e^{i2ka}]/[Z_c\{1 - (\sigma_2/\sigma_1)e^{i2ka}\}]. \tag{38c}$$

**SMALL CONE APPROXIMATION (i.e. $ka << 1$)**

In this case

$$\zeta_n(ka) \simeq -(ka/n) \cdot \left[1 + \frac{(ka)^2}{n(2n-1)}\right] \tag{39}$$

It can be shown also that for $ka << 1$,

$$S \simeq -3Z_0 ka(\cos\psi_1 + \cos\psi_2)^2\Omega(\psi_2)/(8\pi Z_c) + O(ka)^2. \tag{40}$$

Then

$$kh_e(\theta, \omega) \simeq \left[\frac{\Omega(\psi_2)6\pi Z_c(ka)(\cos\psi_1 - \cos\psi_2)}{8\pi Z_c + 3Z_0\Omega(\psi_2)(\cos\psi_1 + \cos\psi_2)^2}\right] \sin\theta. \tag{41}$$

The expression (41) shows that the radiation pattern of a small cone is proportional to sin $\theta$, like a dipole as expected.

$$\begin{aligned} Z_{in} = Z_c \left[\frac{1 - \sigma_2/\sigma_1}{1 + \sigma_2/\sigma_1}\right] &\simeq iZ_c \left[\frac{1 + kaS}{S - ka}\right] \\ &\simeq \frac{(-i8)\pi Z_c^2}{ka[8\pi Z_c + 3Z_0\Omega(\psi_2)(\cos\psi_1 + \cos\psi_2)^2]}, \end{aligned} \tag{42}$$

Here also, as expected, the input impedance of small cone behave like a capacitive impedance $1/(i\omega C_{in})$, where the equivalent capacitance $C_{in}$ can be computed easily from the relation (42). The terminal admittance $Y_{t0}$ can be obtained from (38b) upon substituting (40). Noting that both $Z_c$ and $Y_{t0}$ are functions of $\psi_1$ and $\psi_2$, the following relation can be established easily

$$Z_c(\psi_1, \psi_1)Y_{t0}(\psi_1, \psi_1) = Z_c(\psi_1, \pi/2)Y_{t0}(\psi_1, \pi/2). \tag{43}$$

Since

$$Z_c(\psi_1, \psi_1) = 2Z_c(\psi_1, \pi/2) = (Z_0/2\pi)\ln\left[\cot\left[\frac{\psi_1}{2}\right]\right],$$

it follows then

$$Y_{t0}(\psi_1, \psi_1) = \frac{1}{2} Y_{t0}(\psi_1, \pi/2).$$

Note that the expression (43) and other relations based on it do not depend on the small cone approximation.

**LARGE CONE APPROXIMATION (i.e. $ka >> 1$)**

Let us assume $-1 < \mu_1 \leq \mu_2 < 1$, then we have from [Ref. 46] the following relation.

$$\sum_{\ell=1}^{\infty} \frac{(2\ell + 1)}{\ell(\ell + 1)} P_\ell(\mu_1)P_\ell(\mu_2) = 2 \ln 2 - 1 - \ln[(1 - \mu_1)(1 + \mu_2)], \tag{44a}$$

Replacing then $\mu_1$ by $-\mu_1$ in (44a), noting that $P_\ell(-\mu_1) = (-1)^\ell P_\ell(\mu_1)$, we have

$$\sum_{\ell=1}^{\infty} \frac{(2\ell + 1)}{\ell(\ell + 1)} (-1)^\ell P_\ell(\mu_1)P_\ell(\mu_2) = 2 \ln 2 - 1 - \ln[(1 + \mu_1)(1 + \mu_2)], \tag{44b}$$

$$-1 < -\mu_1 \leq \mu_2 < 1$$

Setting $\mu_2 = -\mu_1$ in (44b) we have

$$\sum_{\ell=1}^{\infty} \frac{(2\ell + 1)}{\ell(\ell + 1)} [P_\ell(\mu_1)]^2 = 2 \ln 2 - 1 - \ln[(1 - \mu_1^2)], \tag{44c}$$

$$-1 < \mu_1 < 1$$

Similarly, write $\mu_1 = -\mu_2$ in (44b) and obtain

$$\sum_{\ell=1}^{\infty} \frac{(2\ell + 1)}{\ell(\ell + 1)} [P_\ell(\mu_2)]^2 = 2 \ln 2 - 1 - \ln[(1 - \mu_2^2)], \tag{44d}$$

Thus substituting (44b) to (44d) appropriately and after some manipulation it can be shown that

$$\sum_{\ell=1}^{\infty} \frac{(2\ell + 1)}{\ell(\ell + 1)} [g_\ell(\psi_1, \psi_2)]^2 = 2 \ln \left[\cot\left[\frac{\psi_1}{2}\right] \cot\left[\frac{\psi_2}{2}\right]\right] \Big/ \Omega(\psi_2) \tag{45}$$

$$= 4\pi Z_c / Z_0$$

Noting also that $\lim_{ka \to \infty} [\zeta_\ell(ka)] = i + O\left[\frac{1}{ka}\right]$, one then finds from (38a) and (45), that

$$\lim_{ka \to \infty} [\sigma_2/\sigma_1] = 0. \tag{46}$$

In order to find the behavior of the effective length of the antenna for large $ka >> 1$, we need the following results. Rewriting (44a) and (44b) we have the relations given respectively (with $\mu = \cos\theta$).

$$\sum_{\ell=1}^{\infty} \frac{(2\ell + 1)}{\ell(\ell + 1)} P_\ell(\mu)P_\ell(\mu_1) = 2 \ln 2 - 1 - \ln[(1 - \mu)(1 + \mu_1)], \quad -1 < \mu \leq \mu_1 < 1, \tag{47a}$$

$$\sum_{\ell=1}^{\infty} \frac{(2\ell + 1)}{\ell(\ell + 1)} (-1)^\ell P_\ell(\mu)P_\ell(\mu_2) = 2 \ln 2 - 1 - \ln[(1 + \mu)(1 + \mu_2)], \quad -1 < \mu \leq \mu_2 < 1. \tag{47b}$$

Differentiating (47a) and (47b) with respect to $\mu$ and noting that $P'_\ell(\mu) = P^1(\mu)$, we have

$$\sum_{\ell=1}^{\infty} \frac{(2\ell + 1)}{\ell(\ell + 1)} P_\ell^1(\mu)P_\ell(\mu_1) = \sqrt{\frac{1 + \mu}{1 - \mu}}, \quad 0 \leq |\mu| \leq \mu_1 < 1, \tag{48a}$$

and

$$\sum_{\ell=1}^{\infty} \frac{(2\ell + 1)(-1)^{\ell}}{\ell(\ell + 1)} P_{\ell}^{1}(\mu)P_{\ell}(\mu_2) = -\sqrt{\frac{1 - \mu}{1 + \mu}}, \quad 0 \le |\mu| \le \mu_2 < 1, \tag{48b}$$

For $ka >> 1$, one finds from Eq. (35) that

$$h_{n-1}^{(2)}(ka) - \frac{n}{ka} h_n^{(2)}(ka) \approx i^n e^{-ika}/(ka). \tag{49}$$

Then from (36b), with the aid of (46) and (48a) is (49), we have

$$\begin{aligned}
&\lim_{ka\to\infty} [kh_e(\theta,\omega)] \\
&= \lim_{ka\to\infty} \left[ \frac{e^{-ika} - (\sigma_2/\sigma_1)e^{ika}}{\{1 + (\sigma_2/\sigma_1)\}\, ka} \sum_{n=1}^{\infty} \frac{(2n + 1)i^{n-1}P_n^1(\mu)g_n(\mu_1, \mu_2)}{2n(n + 1)\left\{h_{n-1}^{(2)}(ka) - \frac{n}{ka} h_n^{(2)}(ka)\right\}} \right] \\
&= \frac{-i}{2} \left[ \sum_{n=1}^{\infty} \frac{(2n + 1)}{n(n + 1)} P_n^1(\mu)P_n(\mu_1) \right. \\
&\quad \left. - \sum_{n=1}^{\infty} \frac{(2n + 1)}{n(n + 1)} (-1)^n P_n^1(\mu)P_n(\mu_2) \right] \\
&= -\frac{i}{\sin\theta},
\end{aligned} \tag{50}$$

Since the right-hand sides of (48a) and (48b) are independent of $\Omega(\psi_2)$, we dropped $\Omega(\psi_2)$ in (50) in this limit of $ka \to \infty$.

Furthermore, it can easily be shown, in view of (46), the input impedance $Z_{in}$ given by (33) becomes

$$\lim_{ka\to\infty}[Z_{in}] = Z_c(\psi_1, \psi_2), \tag{51}$$

which is independent of frequency.

## TIME HISTORY OF THE RADIATED AND THE RECEIVED FIELDS ASSOCIATED WITH WIDE-ANGLE SMALL AND LARGE CONICAL ANTENNAS

The effective length, $h_e(\theta, \omega)$ of an antenna is a useful parameter, which can be used to describe both the transmitting and receiving characteristics of a given antenna. The functional dependence of $h_e(\theta, \omega)$ remains the same whether the antenna is transmitting or receiving. It should be noted, however, that when transmitting $\theta$, the direction of radiation is measured from the axis of the antenna. On the other hand, during reception the angle $\theta$ gives the direction from which the received field is incident and in this case also $\theta$ is measured from the axis of the receiving antenna.

Let $V_g(t)$ be the input source voltage of the transmitting antenna and $\hat{V}_g(\omega)$ is the Fourier transform of $V_g(t)$. If $Z_{in}(\omega)$ and $Z_g(\omega)$ are the input impedance of the antenna and the generator (or

source) impedance, respectively, then the input-current $I(O)$ [or $I(O, \omega)$] and $\hat{V}_g(\omega)$ are related by

$$I(O) = \hat{V}_g(\omega)/[Z_{in}(\omega) + Z_g(\omega)]. \tag{52}$$

The radiated electric field (in the frequency domain) is [see (36a) and (36b)] then given by

$$E_\theta^{rad}(r, \theta, \omega) = \frac{iZ_0}{2\pi}\left[\frac{\hat{V}_g(\omega)}{Z_{in}(\omega) + Z_g(\omega)}\right]\frac{e^{-ikr}}{r}[kh_e(\theta,\omega)]. \tag{53a}$$

The transfer function $T(\omega)$ of the transmitting antenna is defined by

$$\begin{aligned} T(\omega) &= E_\theta^{rad}(r,\theta,\omega)/\hat{V}_g(\omega) \\ &= \frac{iZ_0\omega}{cr}\frac{h_e(\theta,\omega)e^{-i\omega r/c}}{[Z_{in}(\omega) + Z_g(\omega)]}, \end{aligned} \tag{53b}$$

where $c$ is the velocity of light.

Then the time dependent radiated electric field, $e^{rad}(r, \theta, t)$, is given formally by the following inverse Fourier transform.

$$\begin{aligned} e_\theta^{rad}(r, \theta, t) &= 2\pi \int_{-\infty}^{\infty} E_\theta^{rad}(r,\theta,\omega)e^{i\omega t}d\omega \\ &= 2\pi \int_{-\infty}^{\infty} \hat{V}_g(\omega)T(\omega)e^{i\omega t}d\omega. \end{aligned} \tag{54}$$

When the antenna is receiving, we define the open-circuit receiving voltage $\hat{V}_{0c}(\omega)$ by

$$\hat{V}_{0c}(\omega) = -E_\theta^{inc}(r,\theta,\omega)h_\theta(\theta,\omega). \tag{55a}$$

If the receiving antenna is connected to a load with impedance $Z_L(\omega)$, then the received voltage across this load is given by

$$\hat{V}_L(\omega) = -\frac{E_\theta^{inc}(r,\theta,\omega)h_\theta(\theta,\omega)Z_L(\omega)}{[Z_{in}(\omega) + Z_L(\omega)]}, \tag{55b}$$

where $Z_{in}(\omega)$ is the input impedance of the antenna. The impedance $Z_{in}(\omega)$ is the same as that when the same antenna is used for transmitting. One can also define the reception transfer function $S(\omega)$ by

$$\begin{aligned} S(\omega) &= \hat{V}_L(\omega)/E_\theta^{inc}(r,\theta,\omega) \\ &= -\frac{h_e(\theta,\omega)Z_L(\omega)}{[Z_{in}(\omega) + Z_L(\omega)]}. \end{aligned} \tag{55c}$$

Then the time dependent load voltage is given formally by the following relation

$$V_L(t) = 2\pi \int_{-\infty}^{\infty} \frac{\hat{V}_{0c}(\omega)Z_L(\omega)e^{i\omega t}}{[Z_{in}(\omega) + Z_L(\omega)]}\, d\omega$$

$$= -2\pi \int_{-\infty}^{\infty} \frac{E_\theta^{inc}(r,\theta,\omega)h_\theta(\theta,\omega)Z_L(\omega)e^{i\omega t}}{[Z_{in}(\omega) + Z_L(\omega)]}\, d\omega \tag{56}$$

$$= 2\pi \int_{-\infty}^{\infty} E_\theta^{inc}(r,\theta,\omega)S(\omega)e^{i\omega t}d\omega$$

When $\hat{V}_g(\omega)$ and $E_\theta^{inc}(r, \theta, \omega)$ are known, then under different suitable matching conditions, $e_\theta^{rad}(r, \theta, t)$ and $V_L(t)$ can be expressed in closed forms either for $ka << 1$ or $ka >> 1$. Harrison and Williams [38] considered transient radiation from and reception by wide-angle conical antennas above a conducting infinite conducting plane for various special cases for $\theta = \pi/2$. One can revisit all those situations using our general results, which are also valid for all angles $\theta$. Without presenting all of those cases in [38], we shall consider only a few cases as for illustrative purpose.

*Case 1.* We consider first the radiation from a wide-angle short antenna which is matched to the source, i.e. $Z_c = Z_g$. Then substituting (42) for $Z_{in}$ and (41) for $kh_e(\theta, \omega)$ in (53a) or (54) we have

$$e_\theta^{rad}(r, \theta, t) = \frac{\Omega(\psi_2)Z_0 3a^2(\cos\psi_1 + \cos\psi_2)}{Z_c 8\pi^2 c^2 r} \sin\theta \left[\frac{d^2}{dt^2} V_g(t - r/c)\right], \tag{57}$$

in which we have assumed that the following inequality is satisfied for $ka << 1$.

$$|-i8\pi Z_c| >> ka[8\pi Z_c + 3Z_0\Omega(\psi_2)(\cos\psi_1 + \cos\psi_2)^2].$$

The expression (57) shows that for a wide-angle small cone the radiated electric field is proportional to the second time derivative of the retarded input voltage, provided the matching condition $Z_c = Z_g$ is also satisfied. This result is similar to that of a short dipole along which current does not vary spatially.

*Case 2.* As a second example we consider the same matching condition as above, but the antenna now is a long one. In this case we utilize the relations (50) and (51) together with $Z_c = Z_g$ in (54) and obtain.

$$e_\theta^{rad}(r, \theta, t) = \frac{Z_0 V_g(t - r/c)}{4\pi r Z_c \sin\theta}, \tag{58}$$

The result indicates that for a long wide-angle conical antenna the radiated field is an exact retarded replica of the input voltage and the field is maximum along the cone surface with smaller cone angle, i.e. where sin $\theta$ is minimum ($\theta \neq 0, \pi$). This means that such an antenna is an ideal UWB.

*Case 3.* In this case we study the received voltage by a short antenna with its load matched, i.e. for $Z_L(\omega) = Z_c$. Substituting (42) for $Z_{in}$ and (41) for $kh_e(\theta, \omega)$ in (56), we have the following result.

$$V_L(t) = \frac{-\Omega(\psi_2)3a^2(\cos\psi_1 + \cos\psi_2)\sin\theta}{4c}\left[2\pi\int_{-\infty}^{\infty} i\omega E^{inc}(r,\theta,\omega)e^{i\omega\tau}d\omega\right]$$
$$= \frac{-\Omega(\psi_2)3a^2(\cos\psi_1 + \cos\psi_2)\sin\theta}{4c}\frac{d}{dt}[e_\theta^{inc}(r,\theta,r)]. \tag{59}$$

*Case 4.* Here we consider the receiving property of a long wide-angle bicone with matched load (i.e. $Z_L(\omega) = Z_c$). Employing (50), (51) and $Z_L = Z_c$ into the expression (56) we have the following time dependent received load voltage.

$$V_L(t) = -\frac{c}{2\sin\theta}\left[2\pi\int_{-\infty}^{\infty}\frac{E_\theta^{inc}(r,\theta,\omega)}{i\omega}e^{i\omega t}d\omega\right]$$
$$= -\frac{c}{2\sin\theta}\int_{-\infty}^{t} e_\theta^{inc}(r,\theta,\tau)\,d\tau. \tag{60}$$

**REMARKS**

The results presented in this study can be reduced to the corresponding results considered previously by other authors [30-38] as special cases. It is worth noting that the radiated field and the received voltage involving a wide-angle small cone depend explicitly on the cone angles $\psi_1$ and $\psi_2$. However, this is not so for a wide-angle large cone as can be seen from the expressions, (41), (42), (50) and (57) to (60).

It is also interesting to note that in a very recent study Sandler and King [37] made the following observation on the basis of their numerical results:

> "At low frequencies when the antenna is electrically small, the pattern is similar to that of a short dipole .... The maximum radiation occurs at $\theta = \pi/2$. At the higher frequencies where the exit aperture is on the order of a wavelength or larger, the maximum radiation moves away from the horizontal direction and minor lobes appear. As a consequence, the horizontal directivity can decrease at higher frequencies, especially for the larger size bicones."

We can now explain the above numerical behaviors of a bicone for low frequencies via Eq. (41) and for high frequencies via Eq. (50). Since the results of Sandler and King [37], as well as our results, show that maximum radiation does not take place at broadside ($\theta = \pi/2$) for high frequencies, consideration of only the broadside case by Harrison and Williams [38] for $ka >> 1$ is not justified.

We also reproduced some of the numerical results in [37] and discovered a new piece of information, namely, that the infinite series for the far field is very slowly convergent for certain high frequencies. These frequencies may correspond to the electrical resonances of the conical structure. This aspect of radiation problems requires further detailed investigations.

## Appendix B

## RADIATION FIELD OF HELICAL ANTENNAS WITH SINUSOIDAL CURRENT

### SUMMARY

Here we "revisit" the analytical work by E.T. Kornhauser [21]. The assumption of a sinusoidal current distribution is an empirical one which was obtained by Kraus [15]. Kraus found the current distribution experimentally, which can be approximated by a traveling sinusoidal wave whose phase velocity varies with frequency over the useful range so that the radiation pattern maintains a sharply directed beam. The analysis presented here differs from that of Kornhauser, in that we think our expression for the radiated field shows correct variation with the spherical angles $\theta$ and $\phi$.

### METHOD OF ANALYSIS

For the clarity of presentation some notations will be changed. For example, the coordinates of the cylindrical helix of radius $a$ (which are source coordinates) will be primed. Thus we write the equation of the helix as follows [see Fig. 3a and 3b].

$$\left.\begin{aligned} x' &= a\cos\phi' \\ y' &= a\sin\phi' \\ z' &= a\tan\phi' = b\phi' = \frac{p}{2\pi}\phi', \\ &\text{where } p \text{ is the pitch.} \end{aligned}\right\} \tag{1}$$

The pitch angle $\alpha$ is related to $a$ and $b$ in the following manner.

$$\left.\begin{aligned} \cos\alpha &= \frac{a}{\sqrt{a^2+b^2}} \\ \sin\alpha &= \frac{b}{\sqrt{a^2+b^2}} \end{aligned}\right\} \tag{2}$$

Let us assume the traveling wave current distribution along the helix is given by

$$I(s') = I_0 e^{-i\beta_1 s'} = I_0 e^{-i\beta\phi'} \tag{3}$$

where [see Fig. 3b]

$$s'/L = \phi'/2\pi = \frac{a\phi'}{2\pi a} = \frac{z'}{p} = \frac{s' \sin \alpha}{p}, \tag{4a}$$

$$\frac{p}{2\pi a} = \frac{z'}{a\phi'} = \tan \alpha, \tag{4b}$$

$$s' = \frac{b\phi'}{\sin \alpha} = a\phi' \sec \alpha, \tag{4c}$$

$$\beta = \beta_1 \, a \sec \alpha = \omega a \sec \alpha / v, \tag{4d}$$

where v is the phase velocity of the wave along the helix.

Let $\hat{s}$ be the unit vector along the helix. Then we have

$$\begin{aligned} \hat{s} &= (-\hat{x} \sin \phi' + \hat{y} \sin \phi')\cos \alpha + \hat{z} \sin \alpha \\ &= \hat{r}[\cos \alpha \sin \theta \sin(\phi - \phi') + \sin \alpha \sin \theta] \\ &\quad + \hat{\theta}[\cos \alpha \cos \theta \sin(\phi - \phi') - \sin \alpha \sin \theta] \\ &\quad + \hat{\phi} \cos \alpha \cos(\phi - \phi') = \hat{r}S_r + \hat{\theta}S_\theta + \hat{\phi}S_\phi, \end{aligned} \tag{5}$$

where $\hat{x}$, $\hat{y}$, $\hat{z}$, $\hat{r}$, $\hat{\theta}$ and $\hat{\phi}$ are unit vectors along the respective coordinates. The spherical coordinates of the observation point is $(r, \theta, \phi)$. The spherical components of $\hat{s}$ are then given by

$$\left.\begin{aligned} S_r &= \hat{s} \cdot \hat{r} = \cos \alpha \sin \theta \sin(\phi - \phi') + \sin \alpha \cos \theta \\ S_\theta &= \hat{s} \cdot \hat{\theta} = \cos \alpha \cos \theta \sin(\phi - \phi') - \sin \alpha \sin \theta \\ S_\phi &= \hat{s} \cdot \hat{\phi} = \cos \alpha \cos(\phi - \phi'). \end{aligned}\right\} \tag{6}$$

When $\phi' = \phi_0$, let us choose $s' = s_0 = \phi_0 b$ cosec $\alpha$, which follows from (4c). If the helix extends from $-\phi_0$ to $\phi_0$, then $s'$ extends from $-s_0$ to $s_0$.

Let $\vec{r}$ and $\vec{r}'$ be the position vectors of the observation point and a point on the helix, respectively. Then at a large distances, where $|\vec{r}| >> |\vec{r}'|$, we have

$$|\vec{r} - \vec{r}'| = r - \hat{r} \cdot \vec{r}', \tag{7a}$$

$$= r - a \sin \theta \cos(\phi - \phi') - (a \tan \alpha \cos \theta)\phi'. \tag{7b}$$

Then the radiated or far zone electric field of a thin helical wire is given by

$$\vec{E} \approx \frac{i\omega\mu_0}{4\pi r} e^{-ikr} \int_{-s_0}^{s_0} [\hat{r} \times (\hat{r} \times \hat{s})] I(s') e^{ik\hat{r} \cdot \vec{r}'} ds', \tag{8}$$

where $k = \omega/c$ and

$$\hat{r} \times (\hat{r} \times \hat{s}) = -[\hat{\theta}S_\theta + \hat{\phi}S_\phi]. \tag{9}$$

Noting that $ds' = a \sec \alpha \, d\phi'$, the far field components of the electric field can be expressed as follows

$$E_\theta = \frac{i\omega\mu_0 I_0 a e^{ikr}}{4\pi r} e^{i\nu\phi} \left[\tan \alpha \sin \theta \int_{\phi-\phi_0}^{\phi+\phi_0} e^{i(\xi\cos\psi - \nu\psi)} d\psi \right. \\ \left. - \cos \int_{\phi-\phi_0}^{\phi+\phi_0} \sin \psi e^{i(\xi\cos\psi - \nu\psi)} \, d\psi\right], \tag{10}$$

$$E_\phi = \frac{-i\omega\mu_0 I_0 a e^{ikr}}{4\pi r} e^{i\nu\phi} \left[\int_{\phi-\phi_0}^{\phi+\phi_0} \cos \psi \, e^{i(\xi\cos\psi - \nu\psi)} d\psi\right], \tag{11}$$

where

$$\left.\begin{aligned} \xi &= ka \sin \theta \\ \text{and } \nu &= ka \tan \alpha \cos \theta - \beta. \end{aligned}\right\} \tag{12}$$

Using the following well-known relation, the integrals in (10) and (11) can be evaluated

$$e^{i\xi\cos\psi} = \sum_{n=-\infty}^{\infty} i^n J_n(\xi) e^{in\psi}, \tag{13}$$

where $J_n(\xi)$ is the Bessel's function of order $n$ and argument $\xi$.

Thus the radiated electric field components can be expressed in the following manner.

$$E_\theta(r, \theta, \phi; \omega) \approx - E_0(\omega) \left\{ 2 \tan \alpha \sin \theta \left[ J_0(\xi) \frac{\sin \nu\phi_0}{\nu} \right.\right. \\ \left. + \sum_{n=1}^{\infty} i^n J_n(\xi) \left\{ e^{-in\phi} \frac{\sin (\nu + n)\phi_0}{(\nu + n)} + e^{in\phi} \frac{\sin(\nu - n)\phi_0}{(\nu - n)} \right\} \right] \\ - i \cos \theta \left[ J_0(\xi) \left\{ e^{-i\phi} \frac{\sin(\nu + 1)\phi_0}{(\nu + 1)} - e^{i\phi} \frac{\sin(\nu - 1)\phi_0}{(\nu - 1)} \right\} \right. \\ + \sum_{n=1}^{\infty} i^n J_n(\xi) \left\{ e^{-i(n+1)\phi} \frac{\sin(\nu + n + 1)\phi_0}{(\nu + n + 1)} - e^{-i(n-1)\phi} \frac{\sin(\nu + n - 1)\phi_0}{(\nu + n - 1)} \right. \\ \left.\left.\left. + e^{i(n-1)\phi} \frac{\sin(\nu - n + 1)\phi_0}{(\nu - n + 1)} - e^{i(n+1)\phi} \frac{\sin(\nu - n - 1)\phi_0}{(\nu - n - 1)} \right\} \right] \right\}. \tag{14}$$

$$E_\phi(r, \theta, \phi; \omega) \approx E_0(\omega) \left[ J_0(\xi) \left\{ e^{-i\phi} \frac{\sin(\nu + 1)\phi_0}{(\nu + 1)} + e^{i\phi} \frac{\sin(\nu - 1)\phi_0}{(\nu - 1)} \right\} \right. \\ + \sum_{n=1}^{\infty} i^n J_n(\xi) \left\{ e^{-i(n+1)\phi} \frac{\sin(\nu + n + 1)\phi_0}{(\nu + n + 1)} + e^{-i(n-1)\phi} \frac{\sin(\nu + n - 1)\phi_0}{(\nu + n - 1)} \right. \\ \left.\left. + e^{i(n+1)\phi} \frac{\sin(\nu - n - 1)\phi_0}{(\nu - n - 1)} + e^{i(n-1)\phi} \frac{\sin(\nu - n + 1)\phi_0}{(\nu - n + 1)} \right\} \right], \tag{15}$$

where

$$E_0(\omega) = -\frac{i\omega a\mu_0 I_0 e^{-ikr}}{4\pi r}. \tag{16}$$

If the value of $\beta$ is taken as that determined experimentally by Kraus, then it can be seen [21] that only the first one or two terms of the above series expansion of the field components are of any significance. The mathematical reason for this is that for an axially directed beam, $\theta$ is very small and hence $J_n(\xi)$ becomes negligible as $n$ increases.

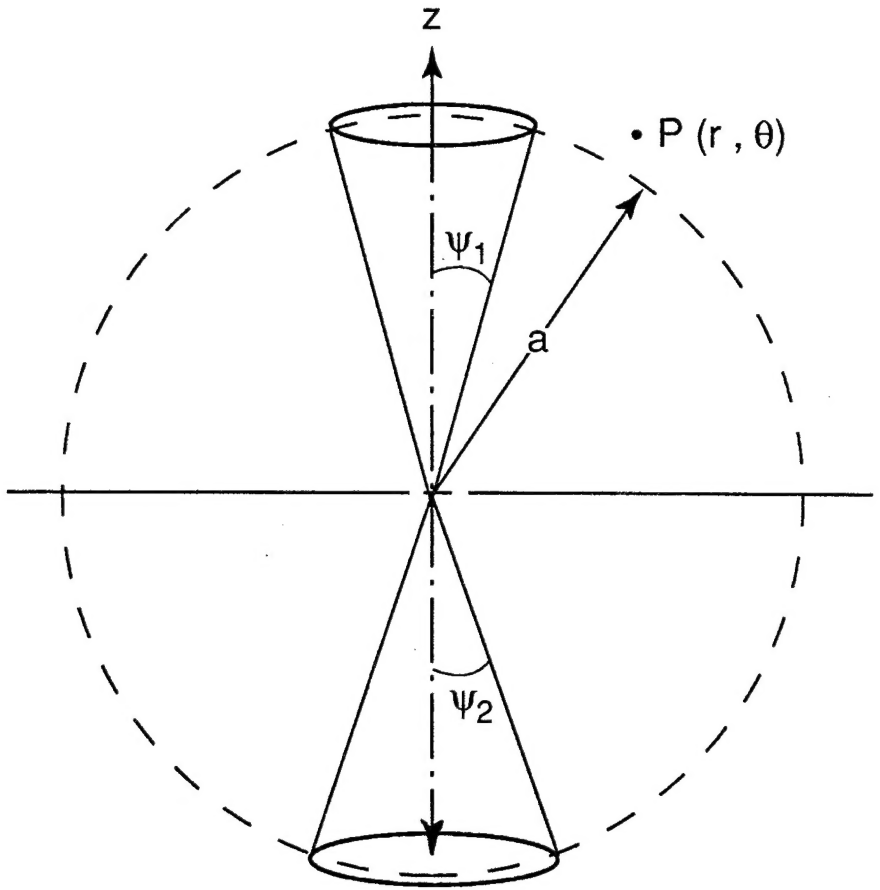


Figure 1 - Spherically Capped Biconical Antenna with Unequal Cone Angles

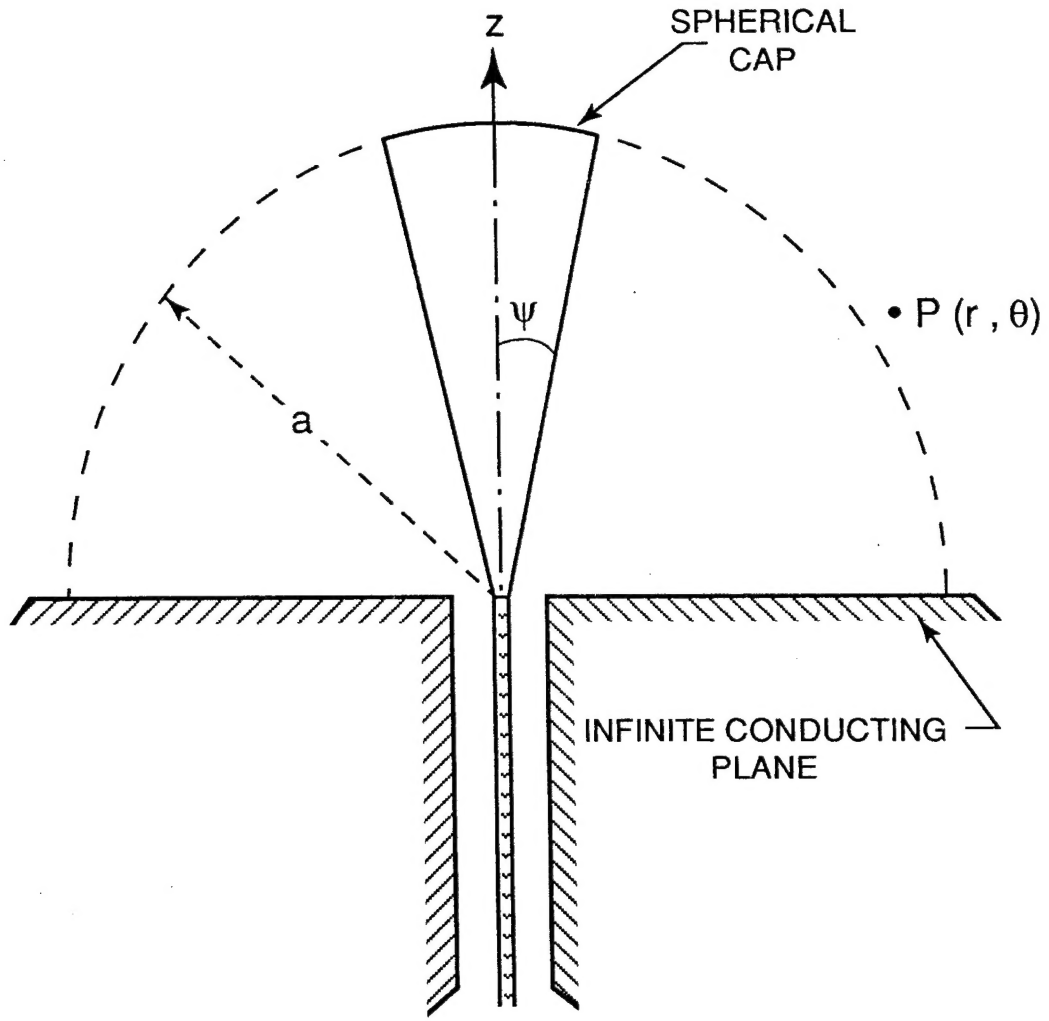


Figure 2 - Spherically Capped Conical Antenna above an infinite Conducting Plane

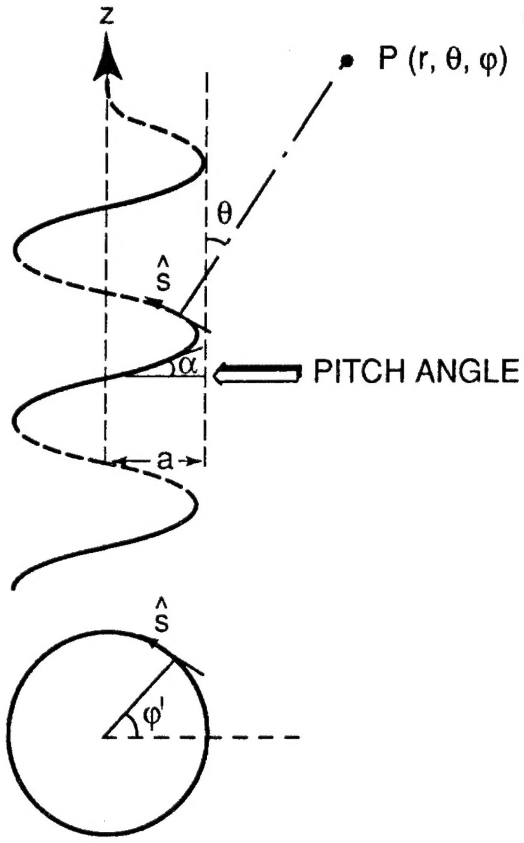


Figure 3a - Helical wire carrying a traveling wave current

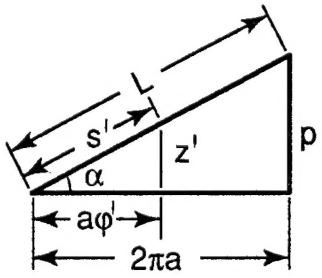


Figure 3b - Some relations involving the helix